LUT
Lappeenranta
University of Technology

Sam Stade

EXAMINATION OF THE COMPACTION OF ULTRAFILTRATION MEMBRANES WITH ULTRASONIC TIME-DOMAIN REFLECTOMETRY

Thesis for the degree of Doctor of Science (Technology) to be presented with due permission for public examination and criticism in the Auditorium 4502 at Lappeenranta University of Technology (LUT), Lappeenranta, Finland on the 10th of November, 2017, at noon.

Acta Universitatis
Lappeenrantaensis 771

Supervisors Professor Mika Mänttäri
LUT School of Engineering Science
Lappeenranta University of Technology
Lappeenranta, Finland

Docent Mari Kallioinen
LUT School of Engineering Science
Lappeenranta University of Technology
Lappeenranta, Finland

Reviewers Professor Emeritus Anthony Fane
School of Chemical Engineering
University of New South Wales
Sydney, Australia

Professor Jack Gilron
The Department of Desalination and Water Treatment
Ben-Gurion University of Negev
Beer-Sheva, Israel

Opponent Professor Jack Gilron
The Department of Desalination and Water Treatment
Ben-Gurion University
Beer-Sheva, Israel

Custos Professor Mika Mänttäri
LUT School of Engineering Science
Lappeenranta University of Technology
Lappeenranta, Finland

ISBN 978-952-335-159-2
ISBN 978-952-335-160-8 (PDF)
ISSN-L 1456-4491
ISSN 1456-4491

Lappeenrannan teknillinen yliopisto
Yliopistopaino 2017

ABSTRACT

Sam Stade

EXAMINATION OF THE COMPACTION OF ULTRAFILTRATION MEMBRANES WITH ULTRASONIC TIME-DOMAIN REFLECTOMETRY

Lappeenranta 2017
88 p.
Acta Universitatis Lappeenrantaensis 771
Diss. Lappeenranta University of Technology
ISBN 978-952-335-159-2, ISBN 978-952-335-160-8 (PDF), ISSN-L 1456-4491, ISSN 1456-4491

Membrane compaction and fouling increases the operational costs of membrane processes and decreases the lifetime of the membrane. Fouling is a major problem in most membrane processes, and it must be considered when membranes, membrane modules and processes are designed and developed. Compaction may also decrease the performance of the membrane process, and wrong operation conditions may damage the membrane permanently. On the other hand, compaction may be beneficial to the membrane process if it densifies the membrane structure and thereby increases its retention. Together, compaction and fouling may have dramatic effects on the viability of the membrane process, and the effects are hard to predict without experimental data.

Ultrasonic Time-Domain Reflectometry (UTDR) can be used to monitor the membrane casting process, compaction, fouling and cleaning in real time and non-invasively. UTDR is based on the detection of the time of flight of the sound waves that are reflected from the membrane surface. However, the usability and accuracy of this technology are very sensitive to changes in the process conditions, such as the temperature, pressure and concentration, due to the fact that sonic velocity is affected by them.

In this thesis, environmental compensation for UTDR has been developed to measure sonic velocity with an additional reference transducer or a double transducer. The double transducer has two sensors at different distances, which allows determination of sonic velocity. UTDR with the reference transducer was found to be more accurate in practical use than UTDR with estimated sonic velocity. Inside the module, integrated transducers seemed to be more sensitive to detecting membrane fouling than measurements through the top plate of the membrane module, which is the common way to use the technique. The developed environmental compensation with transducers integrated inside the module were used to study membrane compaction. Compaction has earlier been studied mostly with offline methods, which lack reversible compaction and permeability information. Online monitoring revealed how different temperatures and pressures affected the reversible and irreversible compaction of different polymeric membranes and their permeability. It was noticed that reversible compaction can be mistaken for concentration polarization as they both have a similar effect on membrane permeability. This may lead to the adoption of inappropriate mitigation methods. Also membrane retention was studied to achieve better understanding of how retention is affected by irreversible compaction of the membrane, and it was confirmed that it was possible to modify membrane retention by pre-compaction of the membrane. It was possible to increase the retentions of all tested membranes by compacting them in higher pressure before use.

Keywords: ultrasonic time-domain reflectometry, membrane filtration, ultrafiltration, environmental compensation, compaction, double transducer

ACKNOWLEDGEMENTS

This thesis study was done at Lappeenranta University of Technology in the Laboratory of Membrane Technology and Technical Polymer Chemistry during 2011-2015.

I wish to express my sincere gratitude to my supervisors Docent Mari Kallioinen and Professor Mika Mänttäri for their advice and collaboration during the study. I want to thank Professor Tuure Tuuva for the many hours of mind breaking discussions of all the new ideas and innovations which came up during these years. I also want to thank Professor Aki Mikkola and Tuomas Hakkarainen for their contribution.

I thank the reviewers of the manuscript, Professor Emeritus Anthony Fane and Professor Jack Gilron, for their valuable comments. It has been an honour to have such prestige reviewers for this thesis.

I also thank the members of the TEKES project NoFoul. There were many fruitful discussions in the project meetings. I am also grateful to all the university personnel who helped me during these years, especially Helvi, Toni, Hate, and other people at "Paja" and "ESK".

I also want to thank my friends at the laboratory who have shared many laughs during these years - Timo, Jussi, Elsi and Jani "J", and the rest of my friends.

My deepest gratitude goes to my parents Marko and Pirkko, who never had a smallest clue on what I was exactly doing during these years.

"Next time I have an idea like that, punch me in the face." -Tyrion Lannister

Lappeenranta, October 17, 2017

Sam Stade

LIST OF PUBLICATIONS

This thesis is based on the following publications, which are referred to in the text by the Roman numerals I-IV.

I **Stade, S.**, Kallioinen, M., Mänttäri, M., Tuuva, T., High Precision UTDR Measurements by Sonic Velocity Compensation with Reference Transducer, Sensors 14 (2014), 11682-11690.

II **Stade, S.**, Hakkarainen, T., Kallioinen, M., Mänttäri, M., Tuuva, T., A Double Transducer for High Precision Ultrasonic Time-Domain Reflectometry Measurements, Sensors 15 (2015), 15090-15100.

III **Stade, S.**, Kallioinen, M., Mikkola, A., Tuuva, T., Mänttäri, M., Reversible and irreversible compaction of ultrafiltration membranes, *Sep. Pur. Technol.*, 118 (2013) 127-134.

IV **Stade, S.**, Kallioinen, M., Tuuva, T., Mänttäri, M., Compaction and its effect on retention of ultrafiltration membranes at different temperatures, *Sep. Pur. Technol.*, 151 (2015) 211-217.

The author's contribution in the publications

I-IV The author planned the laboratory experiments together with the co-authors, carried out the experiments and analysed the data. The publications were written together with the co-authors.

Table of contents

1 Introduction 13

2 Aim and scope of the study 17

3 Outline of the thesis 19

4 Membrane filtration 21

4.1 Pressure-driven membrane filtration processes 21

4.2 Membrane modules 22

5 Phenomena to be monitored 25

5.1 Membrane fouling and concentration polarization 25

5.2 Membrane compaction 26

6 Requirements for online monitoring 29

7 Online monitoring methods 31

7.1 Optical methods 31

7.2 Non-optical methods 34

7.3 Summary of online monitoring methods 37

8 Ultrasonic time-domain reflectometry 39

8.1 Principle of Ultrasonic Time-Domain Reflectometry 39

8.1.1 Time domain 39

8.1.2 Amplitude domain 40

8.1.3 Accuracy 41

8.1.4 Transducer setup 41

8.1.5 Limitations 42

8.2 Examples of use of UTDR in different applications 43

8.2.1 UTDR in monitoring the membrane casting process 43

8.2.2 UTDR in monitoring membrane compaction 44

8.2.3 UTDR in monitoring membrane fouling 44

8.3 Summary of UTDR monitoring 47
9 Materials and methods 49
9.1 Chemicals 49
9.2 Membranes 49
9.3 Equipment 50
9.3.1 Cross-flow filtration equipment with UTDR transducers 50
9.3.2 Three-cell cross-flow filtration setup 56
9.4 Analyses 57
9.5 Filtration experiments 58
9.5.1 Pre-treatment of the membranes 58
9.5.2 UTDR validation 58
9.5.3 Membrane compaction studies with the developed UTDR system 58
10 Results and discussion 61
10.1 Validation of the UTDR equipment 61
10.1.1 Time-domain accuracy of the UTDR setup with a reference transducer 61
10.1.2 Amplitude-domain sensitivity to detect inorganic fouling with transducers integrated inside the module 63
10.2 Membrane compaction evaluation with the developed UTDR system 66
11 Conclusions 73
References 75

SYMBOLS AND ABBREVIATIONS

Symbols

A	amplitude, -
C	sonic velocity, m/s
K	bulk modulus, Pa
s	distance, m
t	time, s
ρ	density, kg/m^3
Z	acoustic impedance, Pa·s/m^3

Acronyms

BSA	Bovine Serum Albumin
CA	Cellulose Acetate
DOTM	Direct Observation Through Membrane
LUT	Lappeenranta University of Technology
MF	Microfiltration
MWCO	Molecular Weight Cut-Off
NF	Nanofiltration
NMR	Nuclear Magnetic Resonance
PES	Polyether Sulphone
PVDF-g-PNIPAAm	Poly(vinylidene fluoride)-graft- poly(N-isopropylacrylamide)
RC	Regenerated Cellulose
RO	Reverse Osmosis
SANS	Small-Angle Neutron Scattering
UF	Ultrafiltration
UTDR	Ultrasonic Time-Domain Reflectometry

1 INTRODUCTION

Membranes are used in a broad range of applications in chemical and environmental technology. Membrane separation processes exploit the ability of the membrane to control the permeation rate of chemical species through it. A setback in membrane filtration is performance decline over time. Fouling and compaction of the membrane typically reduce the efficiency of the membrane process.

Fouling can be minimized by pre-treatment, adjusting the filtration conditions, and cleaning. Pre-treatment is the first step to mitigate fouling by changing the properties of the effluent or by modification of the membrane. During filtration, the pressure, temperature and flow velocity can be adjusted to reduce fouling on the membrane surface. For example, increasing the flow velocity increases turbulence over the membrane, which tends to wash off larger fouling deposits. Mechanical or chemical cleaning can be done during or after the filtration to restore the capacity and separation characteristics of the process (Mänttäri 1997). However, cleaning increases the downtime and costs of the process. Cleaning may cause chemical and mechanical ageing of the membrane, and it must be replaced with a new one eventually (Touffet et al. 2015). Also, compaction may decrease membrane performance irreversibly by increasing its resistance due to densification of the membrane structure (Mulder 1991). Both pressure and temperature increase the compaction of a polymeric membrane. Thus, knowledge of the limits of filtration conditions of polymeric membranes is beneficial for process optimization.

Different monitoring methods have been developed to study membrane fouling and compaction phenomena in laboratory scale. The challenge is the gap between laboratory and field applications. Thus, changes in the state of the membrane are commonly observed from pure water flux measurement. However, pure water flux measurement is not able to differentiate the source of the change, for example compaction or fouling, if they occur simultaneously. If both compaction and fouling can be measured, their effect can be minimized to achieve better overall process efficiency.

Real-time monitoring can be used to improve the efficiency of the membrane filtration process. Monitoring fouling and compaction can help to minimize them by adjusting pre-treatment, filtration conditions, cleaning time and dosage with the help of the information. With real-time monitoring, it is possible to achieve information of the ongoing process and react to changes to postpone the need of cleaning. Early detection of membrane fouling can help to take the

necessary precautions before the removal of fouling will require stopping the separation process for the cleaning cycle. For example, saturated single calcium carbonate ($CaCO_3$) crystals are easier to remove from the membrane surface before they form a thick $CaCO_3$ layer. Monitoring may also reveal the composition of fouling, which helps to decide on the right kind of cleaning chemicals or methods. The cleaning process can be monitored as well, to detect when the membrane is clean, in order to decrease the time of the cleaning cycle, as flux cannot be measured during cleaning (Mairal et al. 2000). The knowledge of the membrane compaction phenomenon monitored in real time gives information of the limits of the membrane; too high a pressure or temperature may damage the membrane permanently, limiting its permeability or the beneficial compaction where the densification of the membrane structure increases its retention. With real-time monitoring, it is possible to measure the compaction phenomenon and link the changes in the permeability and retention of the membrane.

Different kinds of membrane modules and filtration solutions have their own limitations for monitoring methods. For example, optical methods require optical windows and a transparent fluid to be able to function. There are also non-optical methods which can measure through the module, for example X-ray computer tomography and Nuclear Magnetic Resonance (NMR), but they are expensive and complicate methods to use. There are currently available only a few low-cost and easily deployable methods for industrial use. Ultrasonic Time-Domain Reflectometry (UTDR) is one of the monitoring methods that can measure membrane fouling and compaction non-invasively in real time. UTDR is a low-cost acoustic method with transducer price of 100-400 €, and it can be adapted to different modules by mounting the transducer outside the module. It has micrometre-level accuracy and it can be used in systems where optical methods cannot be used, for example with non-transparent fluids.

However, UTDR measurement is sensitive to errors in practical use, where the filtration conditions are not constant. Non-constant filtration conditions affect the sonic velocity in the media where the sound travels, and thereby decrease the measurement accuracy of UTDR remarkably and limit its use in many applications. The problem is solved in this thesis by determining the sonic velocity in the media with an additional reference transducer or a double transducer. The reference transducer or the double transducer measure sonic velocity in real time simultaneously with the UTDR measurement, thus neglecting the effect of process condition changes. The usability of the UTDR setup with a reference transducer or a double

transducer, its accuracy and sensitivity to detect fouling is examined in this thesis, along with membrane compaction studies.

2 AIM AND SCOPE OF THE STUDY

The aim of this study is to improve the usability of the UTDR monitoring method to better understand membrane compaction phenomena. The UTDR is improved in two ways: first with a reference transducer, which allows determination of the sonic velocity in real time. Second, the UTDR transducers are integrated inside the membrane module, which decreases the measurement distance to the membrane surface and thus increases the accuracy and sensitivity of the method to detect fouling, as it is not measured through the module which attenuates the signal. The UTDR transducers integrated inside the module are used to validate the sensitivity of amplitude-domain method to detect inorganic fouling and time-domain accuracy in changing filtration conditions. The improved UTDR system is then exploited in membrane compaction studies to achieve better understanding of membrane compaction phenomena. This reference measurement technology is also integrated into a transducer design to achieve a new double transducer for close-distance measurements in a narrow filtration channel, where there is not enough space for a separate reference transducer.

3 OUTLINE OF THE THESIS

This thesis is divided into a literature part, an experimental part and four journal publications.

The literature part begins in Chapter 4, which describes membrane filtration briefly, including pressure-driven membrane processes and different kinds of membrane modules. Chapter 5 introduces the phenomena to be monitored, including fouling, concentration polarization and membrane compaction. The requirements for the online monitoring method are discussed in Chapter 6. The different online monitoring methods which are comparable with UTDR measurements are presented in Chapter 7. UTDR time- and amplitude-domain methods and where and how they have been used in membrane research are presented in the end of the literature part in Chapter 8.

The experimental part begins with Chapter 9, Materials and Methods, which describes the experimental methods used in this thesis briefly, including the chemicals, membranes, equipment, analyses, and filtration experiments. A more comprehensive description is presented in the publications. Results and Discussion, starting with Chapter 10, presents validation of the developed UTDR setup with the reference transducer and double transducer. The validation includes accuracy testing in constant and changing filtration conditions, and sensitivity testing to detect inorganic fouling. In the end of Chapter 10, the results of the membrane compaction study are summarized, with discussion. The experimental part ends with Chapter 11, conclusions of this thesis.

The publications are enclosed in the end of this thesis. Two of the publications focus on the development of the UTDR method, and two on the membrane compaction study. The focus in publication I is on the development of the UTDR method, to increase its accuracy and measurement possibilities with a reference transducer in different filtration conditions. The double transducer method was continued with the reference transducer idea, and it was validated and presented in publication II. The improved UTDR method with the reference transducer was used to study membrane compaction, and the results were published in two publications (III and IV). Membrane compaction has been mostly studied with offline methods, but they are not able to detect reversible membrane compaction, which was the focus of the third publication (III). The fourth publication (IV) focused on the possible membrane modification with temperature and pressure. Compaction was monitored by using the improved

UTDR method with the reference transducer, and the results were linked to measured flux and retention results.

4 MEMBRANE FILTRATION

Membrane separation occurs in membrane modules where a driving force, for example pressure difference across the membrane is used to force species through a semipermeable membrane. Pressure-driven processes and the different membrane modules typically used in them are presented in this chapter.

4.1 Pressure-driven membrane filtration processes

Pressure-driven membrane filtration is used to separate different suspended solids and dissolved species. Pressure difference across the membrane forces the feed solution through the semipermeable membrane which separates the species that cannot pass it. Separation may occur by the size of the species or some other feature, like charge or diffusivity. The solution passing the membrane is called permeate, and remaining solution concentrate, also known as retentate.

Different membrane processes can be divided into categories by their separation efficiency. Separation efficiency can be described with the membrane pore diameter or the molecular weight of the species which the membrane repels at least by 90 % (Figure 1).

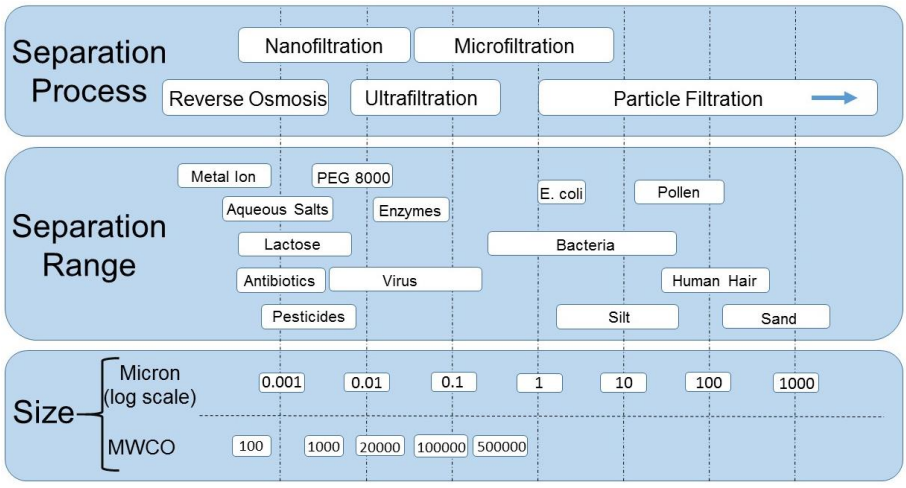

Figure 1. Different filtration processes and their separation efficiency with approximate size and separation range of different species.

The most selective membranes are the reverse osmosis (RO) membranes, which are used for instance in desalination. They can separate water molecules from monovalent ions, such as Na^+ and Cl^-. Nanofiltration (NF) can separate divalent ions, such as Ca^{2+} and Mg^{2+} from water or monovalent ions, and it can be used for instance to remove organic contaminants from water. RO membranes are dense and their separation is affected by diffusivity instead of pore flow. Ultrafiltration (UF) can separate most viruses and enzymes and species bigger than 2-50 nm. Microfiltration (MF) restrains bacteria, yeast and particles bigger than 50 nm. UF and MF membranes are porous, and transport occurs by pressure-driven convective flow through the pores. NF membranes are dense but they may also experience pore flow. (Nunes et al. 2006, Judd 2006, Kennedy et al. 2008)

Pressure-driven membrane processes can be used for instance in water purification (Pervov et al. 1996, Al-Hobaib et al. 2016), waste water treatment (Mersmann 1995, Bazzarelli et al. 2016) and organic solvent separation (Jian et al. 1996, Amirilargani et al. 2016). In food and dairy industry, they are used in the removal of lactose (Goulas et al. 2002, Nordvang et al. 2014), whey (Gésan et al. 1995, Arunkumar et al. 2015) and juice (Jiraratananon et al. 1996, Bagci 2014), as well as beverage clarification (Czekaj et al. 2000, Chimini et al 2016). In pharmaceutical industry, they are used in sterile filtration of pharmaceuticals (Kong et al. 2010, Cao et al. 2016). In biotechnology, they are used in concentration and removal of products in fermentation processes (Solichien et al. 1995, Fu et al. 2016), cell harvesting (Okamoto et al. 2001, Bilad et al. 2014) and virus production (Adikane et al. 1997, Weigel et al. 2016). As a conclusion, membranes are used in many different applications, and it seems that their popularity will increase in the future, as the number of membrane publications is increasing.

4.2 Membrane modules

Several different kinds of modules have been designed for pressure-driven membrane processes. With the right kind of design, it is possible to optimize the hydrodynamics and flow properties of the module and thus minimize the effect of membrane fouling. The packing density and area of the membrane are important parameters for the cost efficiency of the membrane separation process when separation or purification facilities are planned. Also, concentration polarization (CP) must be considered in the planning stage.

In a plate-and-frame module the membrane is located between plates. In the upper plate, there is an inlet and outlet for the feed and retentate, and in the lower plate there is a permeate port.

Also an envelope-type configuration is possible, where two membranes are framed with permeate sides placed together, with a spacer between them. This configuration is easy to use in laboratory-scale experiments, as the membranes can be separated easily for further analysis. The plate-and-frame module is not very popular in the industry, as its packing density is not as great as in spiral-wound or hollow fiber modules. (Böhm et al. 2015, Jhaneri et al. 2016)

Tubular modules are generally limited to MF and UF applications, but there have been also NF applications. The ”membrane” is a pack of tubes or a single tube made of polymer or ceramic material. The feed flows through the tubes and the permeate is collected from the other side of the tube. The advantage of the tubular membrane is that a high content of suspended solids can be processed and the system can be cleaned mechanically. The high flow rate through the module increases turbulence, reducing the fouling tendency. However, the packing density is not as great as in spiral-wound or hollow fiber modules. (Zabkova et al 2007, Kennedy et al. 2008)

In the spiral-wound module structure, two polymeric membrane sheets are placed together, forming an envelope-like structure, wrapped in a spiral shape. The membrane sheets in the envelope are aligned so that the permeate sides are placed together. In the center of the spiral is the permeate collection tube. The feed flows through the spiral tube where there is spacer material between the membranes. The spacer is used to enhance the hydrodynamics inside the spiral-wound structure and to keep the membranes separated from each other. The benefits of this kind of design are good packing density and a large membrane area. (Baker 2004, Karabelas et al. 2015)

Hollow fiber modules are made of a bundle of hollow fibers. There are two types of modules; one where the feed is on the shell side and the permeate flows in the fibers, and one where the feed flows inside the fibers and the permeate is collected from the outside. The benefits of the hollow fiber module are a very large membrane area and high packing density. Also, backwashing is possible during the filtration cycle, which decreases the need of a cleaning cycle. In backwashing, the permeate flow direction is changed so that the permeate pushes the cake layer away, thus cleaning the membrane surface. (Kennedy et al. 2008, Kong et al. 2016)

As a summary, different membrane modules have been made for different applications. Tubular modules can be used with high flow velocities, which reduces their tendency of fouling. Spiral-wound membranes are very common in the industry, as they have good packing

density and a large membrane area. From the monitoring point of view, a spiral-wound module is difficult because the membrane is wrapped inside the shell. Optical methods are not able to monitor through the shell, but non-optical methods have been developed, which can be used instead, for example UTDR. Hollow fiber modules are also problematic, as thin capillary tubes can be difficult to monitor. For instance, fouling can be inside the fiber, which is impossible to view with optical methods and difficult with non-optical methods such as UTDR, where the reflection of the sound wave comes from multiple different fibers and surfaces. The plate-and-frame modules are usable with most monitoring methods, but as their packing density is not as great as in the spiral-wound or hollow fiber modules and they are relatively expensive units compared to the other types of modules, they are used mainly in small-scale applications, such as electrodialysis, pervaporation and some RO and UF applications with highly fouling feed solutions (Baker 2004). However, as a side-stream module, the plate-and-frame module can be suitable for predicting fouling in a spiral-wound module if they have similar filtration conditions (S.T.V. Sim et al. 2015).

5 PHENOMENA TO BE MONITORED

This thesis focuses on the monitoring of membrane fouling and compaction phenomena, which are presented here. Membrane fouling is the biggest challenge in membrane technology. It has been studied for many years to find preventive or mitigative ways to avoid it (Mulder 1991). Even though fouling can be controlled to some extent with different preventive and mitigative methods, the fouling phenomenon is not yet fully overcome. Fouling is often discovered late, when it already affects the flux, and that is why reliable predicative tools are highly interesting for the industry. With real-time monitoring methods, better understanding of the state of fouling and compaction phenomena can be achieved, thereby helping process optimization.

5.1 Membrane fouling and concentration polarization

Concentration polarization (CP) is the accumulation of solutes or particles in the liquid layer near the membrane surface due the convective flux through the membrane. Species that cannot pass the membrane will concentrate near the membrane surface until balance is achieved with back flow of the species in the bulk solution. The CP layer will mix back in the bulk solution when there is no driving force. The CP layer affects the osmotic pressure and resistance to liquid flow through the membrane, which may lead to a change in the flux. CP can be reduced with module design. For example, high turbulence decreases CP, which can be achieved by increasing the crossflow velocity over the membrane and by different kinds of rotating blades and spacers that enhance the shear rate near the membrane surface. CP can enhance fouling, as it can cause for instance supersaturated conditions which enable precipitation of salts (scaling) or sparingly soluble macromolecular species (gel layer) on the membrane surface. (Judd 2003, 2006, Jogdand et al. 2015)

Fouling is deposition and/or adsorption of particles, macromolecules, colloids, and salts on the membrane surface and/or inside the membrane pores and pore walls. Fouling can be divided into organic and inorganic fouling. Particulate fouling is caused by accumulation of soluble organic matter, for instance proteins and polysaccharides on the membrane surface. Biofouling can be categorized as organic fouling where bacteria grows on the membrane surface. Precipitation fouling, also called scaling, is crystallization of solid salts, oxides and hydroxides from water solutions. Fouling may also cause pore narrowing and pore blocking, which reduce the flow through the membrane pores and may affect the selectivity. In adsorption, some species are first attached to the membrane, altering its properties, for example charge, which

may then expose it to fouling, or other foulants may be linked to the adsorbed species, forming a fouling layer. (Judd 2003, Jhaneri et al. 2016)

Fouling increases the resistance of the membrane, which will require a higher driving force, pressure, to achieve the same flux in the process. The increased flux enhances CP and the growth of fouling even further, ending up in a point where it is uneconomic to continue the filtration. To avoid fouling, preventive and repressive measures can be taken. Pre-filters or screens can be used to remove larger particles or highly fouling substances from the feed stream to reduce fouling. High crossflow velocity and turbulence can be achieved with module and spacer design to flush deposits away from the membrane surface. Membrane polymers can be modified to reduce their fouling tendency, for example increase their hydrophilicity. Eventually, the membrane must be cleaned or replaced with a new one. Cleaning is an expense, and it will increase the consumption of chemicals, cause down-time to the filtration process, and shorten the operational life time of the membrane. (Porter 1990, She et al. 2016)

5.2 Membrane compaction

Membrane compaction can be problematic for the separation process if it reduces the permeability of the membrane and thus increases the cost of the process. However, it can also be beneficial if it increases retention due to the densification of the membrane structure. The compaction of polymeric membranes has been studied with static piston-like compression and with hydrodynamic compression (Persson et al. 1995). The effect of the static piston-like compression was studied with offline methods by using a hydraulic press. In static compression, the pressure gradient is same through the membrane and it was noticed to affect the flux more than the hydrodynamic compression. In the hydrodynamic compression, the pressure gradually increases through the membrane with the flux affecting most to the bottom of the membrane and less in the skin layer. Compacted membranes become denser, and the membrane resistance increases with compaction. The increased membrane resistance would require a higher driving force, pressure, to keep up the constant flux, and thereby compaction may increase even further. (Lawson et al. 1995, Persson et al. 1995)

The material and structure of the membrane, and how the load is applied on the polymeric material, all play a role in the extent structural changes occur and how it affects the performance of the membrane. Membrane compaction exhibits viscoelastic behavior rather than simple elasticity. Viscoelasticity involves both time-dependent viscous change and time-independent

elastic change. The latter type of change is recoverable, but the former is not, at least not totally. Viscoelastic changes due to pressure may be characterized as either fast and local or slow and long-range rearrangements of the macromolecules. Also, the reorientation of the bonds on the polymer chain backbone on the atomic scale is temperature- and time-dependent. (Ward 1971, Wineman et al. 2000, Bohonak et al. 2005, Pendergast et al. 2010)

The porosity and asymmetric structure of the membrane complicates the compaction phenomena. Higher porosity in the membrane typically decreases its mechanical strength. Asymmetric membranes may consist of different polymers in different layers of the membrane, amplifying the complexity of the compaction phenomenon by increasing the parameters affecting both the elastic and viscous properties of the membrane. Other known structural factors impacting the mechanical properties of polymers are cross-linking, crystallinity, molecular weight, copolymerization, plasticization, molecular orientation, fillers, blending, and phase separation and orientation in blocks, grafts and blends. (Nielsen et al. 1994, Persson et al. 1995, Wineman et al. 2000, Ebert et al. 2004, Homaeigohar et al. 2012)

The compaction of membranes and different polymers has so far been studied mainly with offline methods. However, the membrane compaction phenomenon studied with offline methods lacks information about thickness changes of the membrane during filtration, known as reversible compaction. When the pressure is released, the membrane recovers partly or fully from the compaction, and thus reversible compaction cannot be seen with offline methods. Also, other real-time data, for instance how fast changes occur during the filtration process, is not accessible with offline methods. There are only a few studies where online methods such as UTDR or electrical impedance spectroscopy have been used to study membrane compaction in real time. (Peterson 1996, Peterson et al. 1998, Reinsch et al. 2000, Aerts et al. 2001, Chilcott et al. 2015)

6 REQUIREMENTS FOR ONLINE MONITORING

A suitable monitoring method must meet some requirements (Figure 2). The parameters of interest for monitoring membrane performance are flux and retention. These parameters can be affected by compaction, CP and fouling, which can be monitored as thickness of the membrane, CP or the fouling layer, and composition. Permeate colour, conductivity and turbidity can be monitored to detect if the membrane is leaking or has defects in the structure.

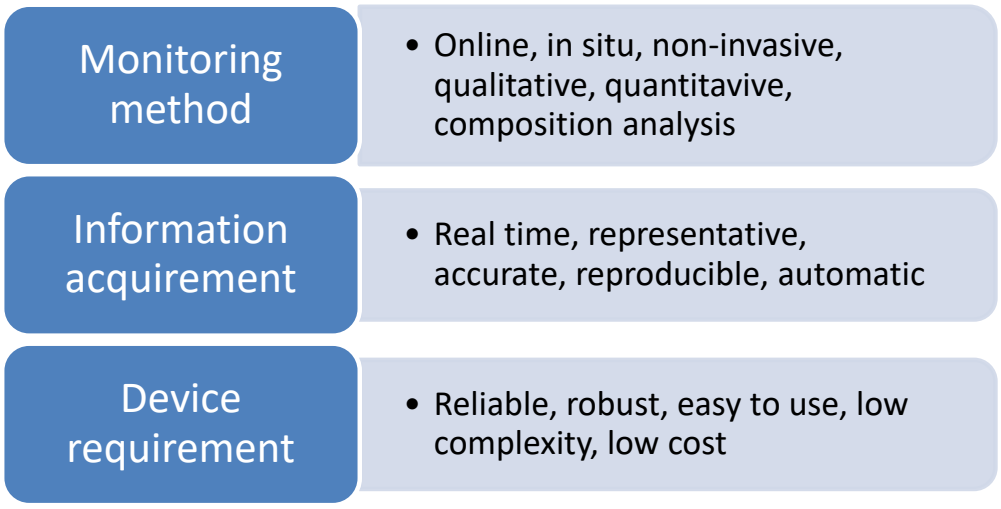

Figure 2. Requirements for monitoring methods.

The monitoring method should be non-invasive, so that the process or product is not affected by the monitoring (Figure 2). This is especially important in drinking water purification and food industry, which are highly regulated industrial fields. Thus, online side stream modules have been designed for monitoring purposes (Vrouwenvelder et al. 2006, 2007, 2009a, 2009b, 2010, 2011a, 2011b, Bartman et al. 2011, Sim et al. 2015). Side stream modules mimic the process conditions of the main stream, enabling the use of different types of monitoring methods without affecting the main process. Different kinds of dyes and tracers for monitoring that cannot be added into the main process, can be added to the side stream module. Fouling layer measurement can be quantitative to understand its extent, or qualitative, which tells if fouling occurs or what type it is. For example, to optimize cleaning, a detailed analysis of the composition can be done to determine what type of fouling occurs, and to what extent. This is important when choosing what kind of a cleaning method and cleaning agents should be used.

The information acquired should be representative, reproducible and accurate, and it should be collected in real time to cover the need of monitoring. Real-time information can be described as information that is representative in an approved time window. For example, if the changes in the process are slow, the information achieved can present a larger time window. The accuracy depends on the monitored parameter. For example, if the fouling particles are the size of microns, it is not necessary to monitor them with nanometre accuracy.

The device requirements for the monitoring method are that it should be reliable, robust and easy to use. Complex equipment requires more knowledge and training, which increases the costs of the monitoring method. Complexity means here the complexity of the equipment and its use. Bigger and more sophisticated high technology equipment can have more parts, and troubleshooting may require a specialist to fix the problems, and the standard user may not be able to do the maintenance. Also, the use of highly complex equipment may need a specialist or a high amount of learning. As an example of equipment of low complexity, a light microscope is simple to use, does not have many exchangeable parts, and maintenance can be done by the user with a manual. For contrast, non-optical equipment like X-ray computer tomography requires a specialist for use and maintenance.

The prices of the monitoring equipment can be divided to inexpensive (<10,000 €), mediocre (10,000-100,000 €) and expensive (>100,000 €). High resolution equipment can be used in laboratories, but they may be too expensive and complicated for standard use in the industrial field. The monitoring method can be expensive and require a specialist to use it if it produces high value to the process. Value can be achieved for example by preventing fouling, postponing cleaning cycles, shortening cleaning cycles, reducing the amount of cleaning detergent, and reducing membrane aging. Large industrial facilities may also have multiple different sites, and the monitoring method may have to be able to cover the monitoring need of all the sites, which favours cheaper equipment or the possibility to install several monitoring probes. The modification of membrane modules for monitoring can be expensive, for example X-ray tomography requires a rotating movement between the sample and the detector (Frank et al. 2000, 2001). Also the process conditions may limit the installation of probes inside the module, for instance high pressure, temperature, alkalinity, or acidity might harm the probe.

7 ONLINE MONITORING METHODS

Some of the existing online monitoring methods that have been used in membrane research and that can be compared with the UTDR are presented in this chapter. More detailed information about these monitoring methods, where they have been used and with what kind of applications, can be found in review articles published in 2004 (J.C. Chen et al. 2004, V. Chen et al. 2004) and a book published in 2009 (Monitoring and visualizing membrane-based processes. Edited by Güell et al. 2009).

7.1 Optical methods

Optical methods are based on light. Light techniques require a transparent solution and some kind of a window or hole for the probe and light beam or source. The optical monitoring methods presented in this chapter are listed in Table I.

Table I Optical methods used to monitor membrane processes. (H. Li et al. 1998, Charcosset et al. 2002, V. Chen et al. 2004, Mendret et al. 2009, Tung et al. 2009, 2012)

Method	Accuracy	Complexity	Price
Direct observation through the membrane	1 µm	Low	Inexpensive
Confocal laser scanning microscopy	0.4 µm	Mediocre	Mediocre - Expensive
Laser triangulometry	5 µm	Low	Mediocre
Photo-interrupt sensor	10 µm / 20 µm *	Low	Inexpensive

* = Closest measurement distance from the membrane

As can be seen in Table I, the accuracy of optical methods varies between 0.4 µm to 10 µm, which are near the resolution of the UTDR (~1 micron). Micron-scale accuracy can detect cake growth and microbial growth, but for example adsorption-type fouling occurs in nanometre scale and is thus out of scope. All optical methods have their limits, and they are discussed in the next paragraphs.

Direct observation through the membrane (DOTM) is an optical method used to study membrane fouling in plate-and-frame MF and UF processes in laboratory scale (H. Li et al.

1998, 2000a, 2000b, 2003, Mores et al. 2001, 2002a, 2002b, Kang et al. 2004, Marselina et al. 2008, 2009). It has a light source on one side of the membrane and an optical microscope with a video camera attached to it on the other side. The light transmitted through the membrane is focused and recorded with the video camera. The method can identify particles larger than 1 μm (H. Li et al 1998). As a requirement, the membrane must be transparent, the feed relatively clear, and the module must have optical windows. The demand of transparent membranes and a clear solution limits the use of this technology. For non-transparent membranes, this technique has been modified to be used above the membrane. This is known as direct visual observation (DVO). It has a video camera (Mores et al. 2001) or a high resolution digital camera (EXSOD-method by M. Uchymiak et al. 2007, 2009) attached to a microscope which takes pictures from the membrane surface through an optical window. However, the solution must still be clear enough to let the light pass. Although these techniques can be used to particle and fluid tracking, and they give a real-time picture of the formation of fouling on the membrane surface in micron scale, it is not capable to measure the thickness growth of the fouling layer, as its depth of detection is limited to a perpendicular video picture. However, later optical coherence tomography (OCT) have been used to study membrane fouling (Gao et al. 2014). Benefit of the OCT is that it can be used to take sub-surface images. Generally, these methods are difficult or impossible to apply on other modules than those of the plate-and-frame type, as it requires a direct path of light to the membrane surface.

Confocal laser scanning microscopy (CLSM) has been used to study membrane fouling (Crespo et al. 1999, Reichert et al. 2002, Dunkers et al. 2003, Marselina et al. 2009, Hassan et al. 2014a,b). It has an epifluorescence microscope and a laser light source. Laser sources have different wavelengths which can be used to emit the specific fluorescent signal of the species. CLSM can be used in two modes: in reflected light or in a fluorescence mode. In the fluorescence mode, fluorescence-labelled or naturally fluorescent fouling species in the feed solution are detected. With CLSM it is possible to reconstruct three-dimensional fouling layers on the membrane or inside the membrane if the light penetrates it. Optical coherence microscopy with interferometric technique can be used with CLSM to monitor highly light-scattering substrates. CLSM has better resolution than a normal microscope, as it can acquire in-focus images from selected depths, and all the scattered and out-of-focus light generated is removed from the imaging. As a downside, this method requires an optical window or a hole for the probe in the module, a light-penetrating solution, and the addition of a fluorescent marker or a naturally fluorescent species in the filtration. Also, the membrane should not be

affected by the fluorescent marker. The maximum resolution has been reported to be ~400 nm (Charcosset et al. 2002). However, CLSM with STimulated Emission Depletion (STED) has reported to have 50 nm x-y resolution and 130 nm axial resolution under optimal conditions (CLSM SP8 GSTED 3x Leica 2015, University of Zurich, online-material). The construction of three-dimensional images from the fouling layers can help understand how the layer grows. The method has gained attention especially in the characterization of biofilm layer formation during membrane filtration of biological matter. Huang et al. (2013) monitored the biofouling of a Southern California seawater RO desalination pilot plant with CLSM. However, the monitoring was not performed in real time. They had an additional membrane module for analysis and monitoring purposes in a side stream where they could remove membranes for CLSM analysis.

Laser triangulometry and laser sheet at grazing incidence (LSGI) technology can be used to measure the height of the cake layer on top of the membrane surface with 5 μm accuracy (Mendret et al. 2009). LSGI is a method similar to laser triangulometry, except that it uses a laser sheet instead of a crude laser spot. It is based on the reflection of laser light from the membrane surface when the fouling layer grows, and it can be detected with a CCD camera. When the cake layer grows, the spot where the reflected light hits the CCD camera changes (Altmann and Ripperger 1997, Ripperger and Altmann 2002). The CCD camera may also be perpendicular to the membrane surface and the laser pointed from the side (Mendret et al. 2009). The method requires a rectangular filtration channel and a transparent filtration cell. Also, the concentration of the suspension limits the use of this method, as in other optical methods which require a transparent fluid. Light diffusion by the high concentration of suspended particles makes the image indistinct (Mendret et al. 2009).

Photo-interrupt sensors have been used to study concentration polarization, fouling phenomena and cake thickness in membrane processes. The method to measure concentration polarization is based on the detection of infrared adsorption in the concentration polarization layer with the electric diode array microscope (EDAM) technique (McDonogh et al. 1995). Tung et al. (2001) applied a similar but a less expensive idea of a high-intensity infrared LED and a high-gain silicon photo-Darlington transistor as a collector. This kind of a design allows a sensor-like design which can be set only one side of the module. W.-M. Lu et al. (2002) used this technique to measure cake thickness. The measurement is based on the detection of voltage change on the detector when the fouling layer grows. The photo-interrupt sensor method can measure

concentration as close as 20 µm (McDonogh et al. 1995) from the membrane surface and the cake thickness can be measured with 10 µm accuracy (Tung et al. 2012).

7.2 Non-optical methods

All the techniques that are not based on light measurements can be categorized as non-optical methods. The non-optical monitoring methods presented in this chapter are listed in Table II.

Table II Non-optical methods used to monitor membrane processes. (L'Hostis et al. 1996, Yao et al. 2005, Yeo et al. 2005, Marselina et al. 2009, V. Chen et al. 2004, Tung 2009)

Method	Accuracy	Complexity	Price
Electrochemical methods	0.2-1 µm	Low	Inexpensive
Impedance spectroscopy	<1 µm *	High	Mediocre
Nuclear magnetic resonance	10 µm	High	Expensive
Radio isotope labelling	20 µm *	Low	-
Small-angle neutron scattering	0.1 nm	High	Expensive
X-ray computer tomography	500 µm	High	Expensive
X-ray microimaging	1 µm	High	Expensive

* = Estimated by V. Chen et al. 2004

As can be seen in Table II, some of these methods are expensive and more complex than most optical methods (Table I). Expensive equipment does not necessarily guarantee better accuracy. Also, more complex equipment often costs more.

Electrochemical methods can be used for velocity mapping, concentration polarization and cake thickness measurements on the membrane surface (L'Hostis et al. 1996, Gaucher et al. 2002a-d, 2003, Cobry et al. 2011a). When there is no cake layer, concentration polarization, velocity and the shear stress profile can be mapped from the electrical response of microsensors. Microsensors are made of inert materials, usually gold or platinum. In cake layer measurements, the microsensor system is first calibrated with bulk suspensions, and then it can be used to measure the diffusion coefficient through the porous cake layer. As a downside, this method requires an active species (e.g. ferricyanide ions, oxygen) in the feed solution, and the

microprobes must be on the membrane surface, which alters the flux and the flow profile, and that is why this is a quasi-non-invasive method. The accuracy of the system depends on the diffusion coefficient of the active species. With ferricyanide ions, the accuracy has been reported by L'Hostis et al. (1996) to be 0.2 µm, and with oxygen 1 µm. Even though the microsensors could be installed inside the membrane module, their lifetime may be reduced and sensitivity to errors increased by the feed, fouling and the cleaning solution.

Impedance spectroscopy has been used in membrane processes with flat sheet membranes, and recently with hollow-fiber membranes (Coster et al. 1992, 1996, L.N. Sim et al. 2013, Bannwarth et al. 2015). The technique is based on applying alternating current across the membrane while varying the frequency and amplitude of the current. The amplitude and the phase difference of the electrical potential across the membrane is measured. It is possible to do both electrical and structural characterization of the membrane by analysing the impedance plots and using models. Conductance and capacitance give information of the multilayer structure of membrane, as well as the fouling, porosity and electrochemical properties of the membrane. Signal analysis is required to model the internal capacitances and resistances of the membrane. Each layer has its unique electrochemical signature, and the change can be detected for instance if fouling occurs. The thickness of a dense membrane can be estimated from capacitance results if the material dielectric constant is known (Coster et al. 1992, Benavente 2009). The method is also suitable for the electrodialysis (ED) process, where it can be used with membrane potential and streaming potential measurements to determine the transport parameters of the membrane, such as ionic permeability (Park et al. 2005, 2006). It has also been used to monitor changes in biological membranes with nanometre spatial resolution (V. Chen et al. 2004). The method is difficult to use with polymeric membranes because of the high impedance of the material (Cen et al. 2015).

The nuclear magnetic resonance (NMR) method has been widely used in different applications in chemical engineering, and is known in medical applications also as magnetic resonance imaging (MRI). The method is based on the excitation and relaxation of protons in an external, highly uniform magnetic field when external radio frequency pulse is applied (Gladden et al. 1994). The radio frequency amplitude, voltage decay and the resonances give information about the monitored chemical environment and the local diffusion coefficient. This technique is commonly used in medical applications to monitor morphological changes in tissues, but it has also been used in membrane filtration to detect flow profiles (Yao et al. 1995, Yang et al.

2014), local concentration polarization (Pope et al. 1996, Yao et al. 1997, Airey et al. 1998), and fouling (Fridjonsson et al. 2015). Paramagnetic species cannot be present when NMR monitoring is used. The signal processing may require a specialist to extract information from it. The method has a rather slow data acquisition time and 10 µm resolution (Marselina et al. 2009).

Radio isotope labelling has been used to measure concentration polarization and membrane fouling in a flat sheet module (McDonogh et al. 1990, 1992, 1995). It is based on the detection of radioactive tracers in a solution. Labelled particles accumulate on the membrane surface and gamma ray emission increases, which can be measured as a voltage change. As an assumption for this technique and the fluorescence method (CLSM), labelled particles are expected to behave as non-labelled particles. This is a very strong assumption, and the technique cannot be categorized as a completely non-invasive method. If the particle is labelled, there is some kind of a tracer particle attached to it, which changes the physical properties of the particle. For example, if the size of the particle is changed, it might not be able to pass the membrane any longer, and accumulates on the membrane surface. Radio isotope labelling requires calibration and analysis of the measurement signal, which complicates the use of the method. Also, high cross-flow velocity may affect the accuracy of the measurement system. The accuracy of the system was not calculated in the original reports (McDonogh et al. 1990, 1992, 1995), but V. Chen et al. (2004) estimated in their review article that the accuracy of this method is 20 µm.

Small-angle neutron scattering (SANS) has been used to monitor membrane fouling with 0.1 nm accuracy (Tung 2009). SANS is based on detecting neutron scattering which may occur by neutron interaction with nuclei, or dipole-dipole interaction with magnetic matter. The method requires a neutron beam source on one side and a detector plane on the other side of the membrane, or the neutron beam can be aligned tangentially over the membrane surface, and the detector plane on the side of the module. Neutron radiation is highly penetrative as neutrons have weak interaction with matter. Silica and alumina membranes are ideal for SANS experiments as they are fairly transparent to neutrons, and the neutron beam can be passed through the membrane (Su et al. 1998, 1999, 2000). For example, it is possible to detect only foulants inside the porous structure of the membrane. SANS can be used also with polymeric membranes which are not as transparent to neutrons (Pignon et al. 2000). In that case, the beam penetrates only the cake layer on the membrane surface, and the foulant structure can be

determined. Even though this method has very high accuracy, it is also a very expensive and complex method.

X-ray Computer Tomography (CT) has been used to study the concentration profile and wetting problems in hemodialyzers (Frank et al. 2000, 2001). More commonly, it has been used to study biological specimens and materials in chemical engineering and geology. The system used for monitoring membranes is similar to the one used in medical applications. It consists of an X-ray source and a detector on the other side of the sample. The reconstruction of the images is done three-dimensionally with a computer. It can be used for larger samples than with the NMR technique, but the spatial resolution is not as good (500 µm, Yeo et al. 2005). X-ray microimaging (XMI) has better 1 µm spatial resolution, and it has been used to measure cake layer and flow characteristics inside the hollow fiber and fouling deposition in the membrane pores (Yeo et al. 2005, Chang et al. 2007). It has a rather slow data acquisition time, and that is why it is not an ideal method for real-time measurements. The changes occurring in the process must be very slow, or otherwise the tomography may not be fast enough to build a representative 3D-image (Remigy 2009). The sample must rotate during the monitoring, and therefore the method is easier to adapt to a hollow fiber than a flat sheet membrane. Also, the non-monitored parts, like the membrane module, must rotate as well and pass the X-ray radiation, which complicates the use of the monitoring method.

7.3 Summary of online monitoring methods

Optical methods are generally less complex and cheaper to use than non-optical methods. However, optical methods require a windowed module or a place for a probe. Also, the membrane and filtrated media may have to be transparent to let light pass. Installation of an optical monitoring method to modules like spiral-wound ones may not be possible, as membrane separation occurs inside the membrane shell, and it may not be possible to apply a windowed structure or light alignment. The best option for optical methods is plate-and-frame modules, where the probes and optical windows can be set near the membrane surface. CLSM is probably the most informative method for naturally fluorescent foulants. It has high resolution and can give 3-dimensional information about the fouling layer. However, fluorescent and radio isotope labelling might not be very desirable for industrial processes, as it might affect the product or process itself. However, there could be a side-stream monitoring module where similar membrane and filtration conditions are used with fluorescent labelling. This could be used as a predictive method and to give some insight into the ongoing state of

fouling in the main process. Laser triangulometry and a photo-interrupt sensor can measure cake layer thickness from the top of the membrane. This kind of a measurement setup is similar to the one used in UTDR measurements. However, laser triangulometry and the photo-interrupt sensor are limited by the transparency of the solution, and they require a window or a hole for a probe. UTDR does not have these limitations, and it has 0.75-micron resolution, which is 5- to 10-fold better than the resolution of laser triangulometry or the photo-interrupt sensor (Table I).

Interesting non-optical methods are electrochemical sensors and probes which can be installed in the structure and design of the membrane module. However, the installation should be done by the manufacturer to pass all the regulations and to be easy to use. Also, impedance spectroscopy is an interesting method if it is possible to install the probes or sensors near the membrane surface. It is problematic for polymeric membranes, however, as they have high impedance, which complicates the use impedance spectroscopy. Methods such as NMR, SANS and X-ray topography are too expensive and complex to be used as common monitoring tools in different processes. Also, the slow data acquisition time may limit the use of a method as real-time measurement, for example as in X-ray topography. UTDR has 10-fold better resolution than NMR, it is cheaper and not as complex a method to use. SANS has very good resolution, 0.1 nm, but it comes with a very high price, and depending on what kind of application the monitoring method is used for, the 0.75 µm accuracy of the UTDR method could be sufficient.

8 ULTRASONIC TIME-DOMAIN REFLECTOMETRY

Considering the advantages and disadvantages of the monitoring methods presented in the previous chapter, Ultrasonic Time-Domain Reflectometry (UTDR) is a potential option in membrane monitoring methods. It can be used with solutions which are non-transparent to light, which limits use of optical methods, and its use does not necessarily require any modification of the module. 0.75 µm (Petterson et al. 1998) accuracy is decent compared to other monitoring methods, and UTDR is not an expensive or complicated method to use.

UTDR was introduced to membrane technology in the mid-1990s (Bond et al. 1995). It has been used to measure membrane compaction (Peterson et al. 1998), membrane casting process (Kools et al. 1998), and fouling and cleaning in different processes (Mairal et al. 2000, J. Li et al. 2002a, 2002b, 2002c, 2006, Zhang et al. 2003, Liu et al. 2006). UTDR has also been used in many industrial, medical and military applications (Lynnworth 1989, M.L. Sanderson et al. 2002).

8.1 Principle of Ultrasonic Time-Domain Reflectometry

Ultrasonic time-domain reflectometry is based on time-of-flight (time domain) and/or amplitude change measurements (amplitude domain). The amplitude-domain method is sensitive to detecting changes in different interfaces of the membrane, for example the membrane/fouling interface. The time-domain method measures the distance to the surface. Both methods have their own drawbacks, for example the distance measurement is sonic velocity -dependent. The filtration conditions affect the sonic velocity, and this should be considered when the monitoring system is used. This is a limiting factor in the use of this method in processes where the filtration conditions or the bulk solution may change.

8.1.1 Time domain

An ultrasonic transducer consists of a piezoelectric crystal which can send and receive high frequency sound waves. When an electrical pulse from the pulser is sent to the crystal, it starts to vibrate and a mechanical sound wave is formed. When the sound wave encounters a surface, part of the sound wave energy is reflected and part of it continues traveling in the matter. When the reflected wave returns to the transducer, the crystal starts to vibrate, and it can be detected with an oscilloscope as a voltage change. Examples of the UTDR signals are shown in the Figure 3 in the Publication II. The time between the sent and received signal can be measured

and linked to the path which the sound travelled. If the sonic velocity (C) is known, the distance between the transducer and the target surface (Δs) can be calculated from Equation 1:

$$\Delta s = \frac{C\Delta t}{2} \tag{1}$$

where Δt is the measured arrival time of the ultrasonic echo.

The sonic velocity (C) for the fluids can be written in general as:

$$C = \sqrt{\frac{K}{\rho}} \tag{2}$$

where K is the bulk modulus and ρ is the density of the fluid. The bulk modulus can be described as the fluid volumetric elasticity, and it is defined as the volumetric stress per the volumetric strain.

In fouling measurement, first the distance to the clean membrane is measured. After that, a change in the distance is assumed to be from the fouling layer. The time of the reflected echo decreases as the fouling layer grows. Compaction is measured similarly, except that the distance change is contrary; the time of the reflected echo increases as the membrane compacts and the distance between the transducer and the surface increases (Bond et al. 1995). These two phenomena, compaction and fouling, compensate each other, which complicates use of UTDR as fouling monitoring. One way to avoid this is to compress the membrane at high pressure before the fouling measurement to compact the membrane, and then take the reading of the compacted membrane as the starting value for the fouling measurement. However, slow viscous membrane compaction may still occur during the fouling measurement.

8.1.2 Amplitude domain

UTDR can be used in fouling measurement as an amplitude-domain method as well. It is based on the acoustic impedance difference between two media. When the acoustic wave encounters the interface between these two media, the energy of the wave is partitioned between a reflected wave and a transmitted wave. The reflected or the transmitted wave can be monitored, and the amplitude is the ratio between the reflected/transmitted wave and the incident wave, given by Equation 3:

$$A = \frac{Z_1 - Z_2}{Z_1 + Z_2} \tag{3}$$

where Z_1 and Z_2 are the acoustic impedances of the two media which can be calculated by $Z=\rho C$, where ρ is density and C is the sonic velocity in the media (Reinsch et al. 2000). The greater the impedance mismatch between the two media is, the greater percentage of the energy of the incident wave is reflected at the interface. Therefore, even small changes in the acoustic mismatch can give information about the state of the ongoing process.

8.1.3 Accuracy

The accuracy of the UTDR time-domain method has been reported to be 0.75 µm, based on 1 ns measurement accuracy in determination of the time of flight (Peterson et al. 1998). However, Reinsch et al. (2000) report problems due to temperature control in membrane compaction studies with high-pressure gas. They report a 7 µm error due to 1 °C temperature change on a 2.8 mm roundtrip from the transducer to the membrane and back. Similar problems may occur with fluid filtration. Reinsch et al. (ibid.) suggest that temperature control is necessary in UTDR experiments. They also report that their measurement system expanded at 2.77 MPa pressure by 25.6±4.2 µm. At 0.92 MPa their measurement system expanded by 7.0±1.9 µm. Karjalainen (2010) had similar problems with the module used in his studies. Even small changes in module dimensions during UTDR measurements influence the measurement accuracy significantly. The accuracy of the amplitude domain is measurement system and application -specific, and accuracy is generally not reported in amplitude domain measurements.

8.1.4 Transducer setup

The transducer can be mounted outside the module (Figure 3) with a coupling agent, which can be a high-viscosity fluid like petroleum jelly or honey (Kools et al. 1998, Mairal et al. 1999). Measurement through the membrane module decreases the sensitivity of the amplitude-domain method, as the measurement distance and the number of reflective surfaces which the sound must travel through increases. Also the measurement error of time-domain method increases as the measurement distance increases. Thus, mounting the transducer as close as possible to the monitored surface is beneficial. Cobry et al. (2011b) attached the transducer inside the module under the membrane, which seemed to be more sensitive to detect scaling on the membrane surface. This allowed measurement without a coupling agent, as the transducer was immersed in the solution. Also, the sound wave did not have to go through the top plate which would scatter it.

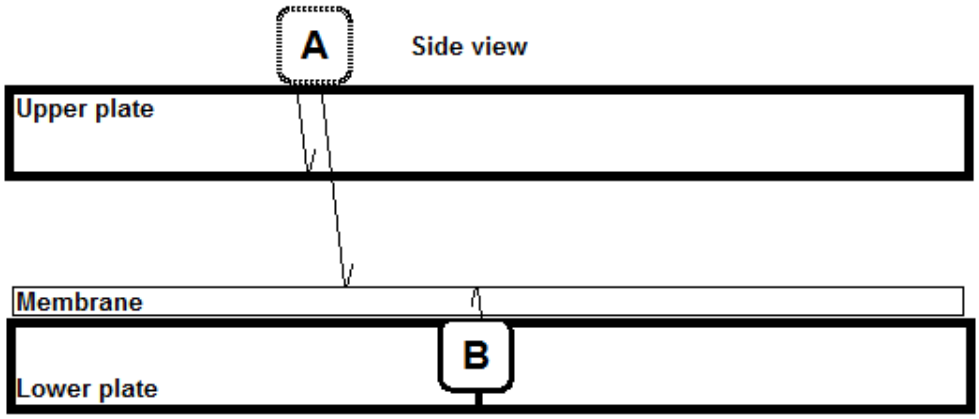

Figure 3. Different ways to position the transducer to a plate-and-frame module; transducer A is mounted outside the module, which is the common way to attach the transducer, and transducer B is integrated inside the module under the membrane (Cobry et al. 2011b).

8.1.5 Limitations

The challenge in the UTDR time-domain method is the changing filtration conditions. Changes in the filtration conditions affect the sonic velocity, which has a significant impact on measurement accuracy. It is known that pressure does not have as big an impact on sonic velocity in a fluid, for example water, which is almost incompressible. However, the temperature affects the sonic velocity in fluids greatly. Also changes in the concentration may affect the sonic velocity if the density of the medium changes. Keeping all filtration conditions constant is difficult in practical use, which limits the use of UTDR in different applications.

A problematic issue in amplitude-domain method measurement is that the morphology of the surface affects the signal scattering and thus the sensitivity of the system (Peterson et al. 1998). As amplitude-domain measurement is simply based on signal attenuation or intensification, changes which may affect in sound reflection or traveling may cause measurement error. Measurements through the top plate also attenuate the signal, which decreases its sensitivity in amplitude-domain measurements, as each layer which the sound must travel through will scatter some of the sound energy. Transducers can be mounted inside the module, but then they are exposed to the filtration solution and conditions which may affect the lifetime of the transducer.

Acoustic impedance (Z) is sonic velocity and density -dependent; it may cause error in amplitude-domain measurements if the sonic velocity is not constant or the density of the medium changes, for example, if the temperature of the medium or the membrane changes. Also compaction of the fouling layer or a porous membrane increases the density of the material and affects sonic velocity. Porous membranes consist of membrane material and fluid in the pores of the membranes. Compaction decreases the porosity, and thus the membrane density increases. Similarly, the sonic velocity of the porous membrane is a combination of the sonic velocity of the membrane material and the fluid. Compaction decreases the fluid portion of the porous membrane, and thus the overall sonic velocity increases as the sonic velocity of the solid membrane material is higher than that of the fluid.

8.2 Examples of use of UTDR in different applications

UTDR has been used to measure the membrane casting process, compaction and fouling, which are presented in this chapter.

8.2.1 UTDR in monitoring the membrane casting process

Metters (1996) presented in his master's thesis a way to monitor membrane solidification in the casting process. Later, Kools et al. (1998) used a similar technique to monitor the casting of cellulose acetate (CA) membranes. They had the transducer directly under the aluminium plate where a casting knife was used to control the thickness of the casted membrane. They could monitor the peaks in the casting substrate/solution, the solution/solidified layer and the solidified layer/gas phase. Detection of the solution/solidified layer was problematic as the reflected echo was mixed in other echoes (casting substrate/solution and solidified/gas phase). The resolution for this kind of measurement was expected to be ±5 µm (Kools et al. 1998). Also Feng et al. (2012) used UTDR to monitor the casting process of a poly(vinylidene fluoride)-graft- poly(N-isopropylacrylamide) (PVDF-g-NIPAAm) thermo-sensitive membrane, and Zhao et al. (2015) the casting of a calcium alginate hydrogel filtration membrane. This kind of monitoring enables determination of the solidification time of the whole membrane, which is not possible with optical methods from the top of the membrane. Amplitude changes reveal when the solidification process has ended, and this enables optimization of the solidification time. However, the temperature and composition of the monitored membrane cause error in the thickness determination if they are not kept constant, which may be difficult in practise.

8.2.2 UTDR in monitoring membrane compaction

There are only a few published compaction studies made with UTDR. First, Bond et al. (1995) introduced UTDR as a new method which can be used for in situ real-time characterization of membrane compaction and fouling. Bond et al. noticed that a 150 µm thick BW-30 membrane compacted to 135 µm, and as the selective layer was only 0.2 µm, most of the compaction occurred in the porous support layer of the membrane. Later Peterson (1996) made a master's thesis titled "Use of acoustic TDR to assess the effect of crosslinking on membrane compaction", where he studied how different operating pressures, porosity and crosslinking affected the compaction of dry-casted cellulose acetate (CA) membranes in real time. The results were obvious: pressure and porosity increased compaction and crosslinking reduced it.

Reinsch et al. (2000) studied how compaction affects the performance of gas separation membranes. They noticed that compaction increased when the feed gas contained CO_2, which works as plasticizer for the CA membrane they used. They also noticed the need of temperature control in their studies. Temperature affects the sonic velocity and thus the measurement accuracy, as they expected sonic velocity to be constant in their measurements. They report a 7 µm error due to 1 °C temperature change on a 2.8 mm roundtrip from the transducer to the membrane and back.

Aerts et al. (2001) studied how filler concentration of zirconia (ZrO_2) particles affects the compaction of polysulphone ultrafiltration membranes. They noticed that when the filler concentration increased, the elastic compaction decreased, but the time-dependent viscoelastic compaction increased. They also observed a permeation decline, which was assumed to be from compaction of the skin layer, and suggested additional experiments to study this relationship.

Based on the available literature, UTDR is very suitable for membrane compaction monitoring in real time if the filtration conditions are kept constant. Changing filtration conditions will cause error in the measurements and thus limit the use of this method.

8.2.3 UTDR in monitoring membrane fouling

Most of the UTDR studies related to membrane technology have focused on fouling experiments. Most UTDR studies cover MF, UF, NF and RO processes, and one publication concerns gas separation membranes. UTDR measurements have been done mostly in plate-

and-frame modules but also spiral-wound, tubular and hollow fiber modules have been used (Mairal et al. 1999, 2000, Reinsch et al. 2000, J. Li et al. 2002a, 2002b, 2002c, 2003, 2006, 2015, Liu et al. 2006, An et al. 2011). The plate-and-frame module is easiest to measure, as the flat surface reflection can be easily recognized from the signal, whereas the signal from a spiral wound module is more difficult, as there are multiple reflections from different layers of the spiral wound membrane. Also, the tubular, spiral-wound and hollow fiber surfaces are curved, which causes scattering of the signal. Lately UTDR monitoring has been used to control fouling with a flow-reversal setup (Mizrahi et al. 2012, X. Lu et al. 2012) and to predict fouling in a side-stream module (S.T.V. Sim et al. 2015, Taheri et al. 2013). The use of UTDR in fouling monitoring is presented in Figure 4.

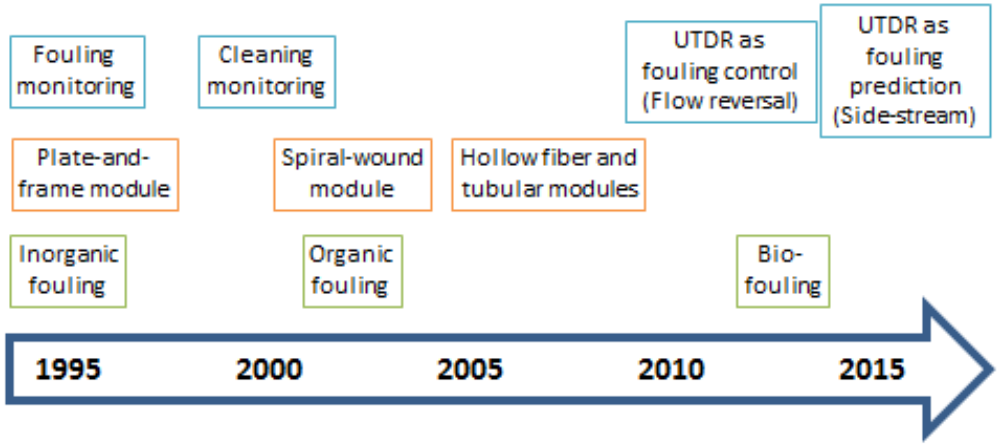

Figure 4. Timeline of UTDR monitoring of membrane applications. (Bond et al. 1995, Mairal et al. 2000, J. Li et al. 2002a, 2002b, 2002c, 2006, Zh.-X. Zhang et al. 2003, Liu et al. 2006, Mizrahi et al. 2012, X. Lu et al. 2012, S.T.V. Sim et al. 2013, 2015, Taheri et al. 2013)

The foulants used in UTDR studies vary between inorganic and organic ones. Typical inorganic foulants are kaolin (J. Li et al. 2002c, Xu et al. 2009), colloidal silica (Chong et al. 2007, S.T.V. Sim et al. 2012, 2013, 2014), NaCl (Taheri et al. 2013, S.T.V. Sim et al. 2014, X. Li et al. 2015), $CaSO_4$ (Bond et al. 1995, Mairal et al. 1999, 2000, J. Li et al. 2005, Z. Zhang et al. 2006, An et al. 2011, Cobry et al. 2011b, X. Lu et al. 2012), and $CaCO_3$ (R. Sanderson et al. 2002, J. Li et al. 2007, Mizrahi et al. 2013). Colloidal silica has been used as an acoustic enhancer when NaCl, organic or biofouling have been examined, because it enables improved detection of organic fouling with UTDR (Taheri et al. 2013, S.T.V. Sim et al. 2013). Time-domain detection of organic and biofouling can be challenging, as for example the acoustic impedance of

bacterial cells is close to that of water, and thus no strong reflection from water-bacterial cell surface cannot be achieved. Fouling monitored mainly with the amplitude-domain method includes paper mill effluent (J. Li et al. 2002a,b, 2003), BSA (J. Li et al. 2005, 2006, X. Li et al. 2015), oily water or wastewater (Liu et al. 2006, Silalahi et al. 2009), canola oil (J. Chen et al. 2014), yeast suspension (X. Li et al. 2012, 2013, 2014a, 2014b), humic acid solution (Lin et al. 2013), and biofouling (S.T.V. Sim et al. 2013). Inorganic fouling is usually easier to detect with amplitude and time domain, as the acoustic mismatch of the fouling layer is higher with a water/inorganic and inorganic/polymeric membrane surface than with a water/organic or biofouling layer/membrane surface.

The amplitude-domain method has been used more often than the time-domain method in fouling studies. Mairal et al. (2000, p. 59) report that the amplitude-domain method provides "as good a measure of fouling layer growth as flux-decline behavior". This is a very strong statement, as amplitude measurements provide information from a small area of the membrane surface and flux measurements from the whole membrane area. Furthermore, the amplitude-domain method as fouling monitoring is based on intensification or attenuation of the signal by fouling. However, other factors may also affect the signal, for example changes in the density of the medium. This can easily lead to misinformation in amplitude-domain measurement. However, in the cleaning process, amplitude measurement can provide useful information, as flux may not be measured during the process. The cleaning process is often completed by standardized time which is known to be sufficient to clean the membrane. With UTDR it is possible to measure the state of the cleaning process in real time and thus save time. J. Li et al. (2002c) reported that SEM (Scanning Electron Microscopy) and permeation studies were in good agreement with amplitude-domain results in membrane cleaning of kaolin fouling in an MF process. Similar results with inorganic fouling ($CaSO_4$ and $CaCO_3$) and cleaning experiments are reported by Mairal et al. (2000) and R. Sanderson et al. (2002) for the RO membrane process. Later, J. Li et al. (2003) report UTDR to be able to measure also the fouling of paper mill effluent and cleaning in a UF membrane process. They also state that the signal amplitude could give quantitative information of the density of the fouling layer. The density of the fouling layer with time-domain thickness data provides information of the state of the fouling layer.

UTDR with amplitude-domain measurements has been used to control an ongoing fouling process. X. Lu et al. (2012) report how real-time UTDR information can be used to control the

flow direction in the RO module. Changing the flow direction decreased $CaSO_4$ scaling over time. A similar study is reported of by Mizrahi et al. (2012), except that they used $CaCO_3$ as the foulant. This kind of "smart" monitoring and controlling devices can be used to optimize the performance of the process. However, the usability of this kind of a system in industry may be error-sensitive, as the filtration conditions are not as controlled as in experiments. For example, temperature changes may cause error measurements which escalate in unnecessary flow direction changes, thereby reducing the efficiency.

S.T.V. Sim et al. (2015) used UTDR in a side-stream module to predict fouling in an ongoing RO process. A spiral-wound membrane was cut open and set in a side-stream plate-and-frame module (curved membrane with spacer set in flat form). The side-stream module had the same kind of flow conditions as the main process stream. The results of the prediction of the ongoing fouling were in good agreement with the main stream fouling in the real process. This kind of a setup could be used for an early warning system in industrial plants. It is unclear how error-sensitive this kind of a system is if the filtration conditions or the composition of the foulants change during the filtration. Predicative tools can be error-sensitive to quick changes, as prediction is often based on a history of statistics and algorithms which have been determined earlier.

8.3 Summary of UTDR monitoring

UTDR monitoring has many advantages as a non-invasive real-time monitoring system for membrane applications. As a non-invasive method, UTDR requires no markers or labelling, as radio isotope labelling or the CLSM method with labelling do. UTDR can be used in real time, which means that it can be performed simultaneously with an ongoing process. Hence, the state and progress of the fouling or cleaning process can be determined (R. Sanderson et al. 2002). Also the change in the membrane thickness may be linked to the porosity of the membrane and the average pore size (Peterson et al. 1998). 0.75 µm accuracy is good compared to other methods in the same price category. The technique is easy and inexpensive to use; transducers do not cost much, which enables them to be installed in multiple locations, and using the system does not require more training than the use of PC software with an oscilloscope. The UTDR transducer can be mounted outside the existing module via a coupling agent, which is usually a high-viscosity fluid, or it can be integrated inside the module and coupled with the feed or permeate, and no optical window or transparent module is needed (R. Sanderson et al. 2002,

Cobry et al. 2011b). Sound also travels through non-light-permitting fluids which cannot be monitored with optical systems.

One of the challenges of UTDR monitoring is that sonic velocity changes can affect measurement accuracy. The temperature, pressure and concentration may change the sonic velocity, and they should be kept constant during measurements, which can be impossible in practice in the industry. Time- and amplitude-domain changes may be hard to detect from layers which have small differences in acoustic impedances, for example biofouling. In biofouling, the bacterial cells are mostly water, which does not have great difference in acoustic mismatch with water solutions, and thus they barely reflect the sonic wave to be detected. The modules may be difficult to monitor if there are many reflective surfaces which scatter the sound wave and attenuate the signal. Some of these challenges can be solved, for example sonic velocity can be measured with an additional reference transducer, which is presented in this thesis.

9 MATERIALS AND METHODS

The experimental materials and methods applied in this study are summarized here. A more detailed description is given in publications I-IV.

9.1 Chemicals

The chemicals used in the experiments are presented in Table III. Polyethylene glycol (PEG) was chosen for retention studies (publication III-IV) to determine membrane selectivity before and after the membrane is compacted. A calcium carbonate ($CaCO_3$) layer was formed with calcium chloride ($CaCl_2$) and sodium bicarbonate ($NaHCO_3$) to study the sensitivity to detect an inorganic fouling layer.

Table III. Model compounds used in the experiments.

Manufacturer	Substance	Used in
Fluka	PEG 6000	Retention experiments, publication III-IV
Sigma-Aldrich	PEG 8000	Retention experiments, publication III-IV
Merck	$CaCl_2$	Inorganic fouling sensitivity testing
Merck	$NaHCO_3$	Inorganic fouling sensitivity testing

PEG = Polyethylene glycol

9.2 Membranes

The membranes used in the experiments are presented in Table IV. In this study, UF membranes were used in compaction experiments in publications III-IV, an NF membrane Desal-5 DK was used to test the sensitivity of the UTDR equipment to detect inorganic fouling.

Table IV. Properties and limitations of the membranes used in the experiments, as provided by the manufacturers.

Manufacturer	Membrane	Selective skin layer	Backing material	MWCO** (g/mol)	Max temp. (°C)	pH-range	Used in
GE Osmonics	Desal-5 DK	PA	PSf	150-300	50	3-9	Inorganic fouling sensitivity testing
Microdyn-Nadir	UC030	RC	PET	30000*	55	1-11	Publication III-IV
Microdyn-Nadir	UH030	PESH	PE/PP	30000*	95	0-14	Publication III-IV
Microdyn-Nadir	UP020	PES	PE/PP	20000*	95	0-14	Publication III-IV
Vladipsor	C30V	RC	PE/PP	N/A	70	2-13	Publication III-IV

* As measured by Microdyn-Nadir (at 3 bar, 20 °C, stirred cell 700 rpm, water fluxes: UH030 >100, UP020 >200 and UC030 >300 L/(m^2h))

** MWCO refers to the lowest molecular weight which is retained 90 % by the membrane.

9.3 Equipment

Two different filtration setups were used in the study; a cross-flow filtration setup with UTDR transducers and a three-cell cross-flow filtration setup.

9.3.1 Cross-flow filtration equipment with UTDR transducers

The UTDR equipment was connected to a crossflow filtration system which was used in all the experiments where time- or amplitude-domain measurements were done (Figure 5).

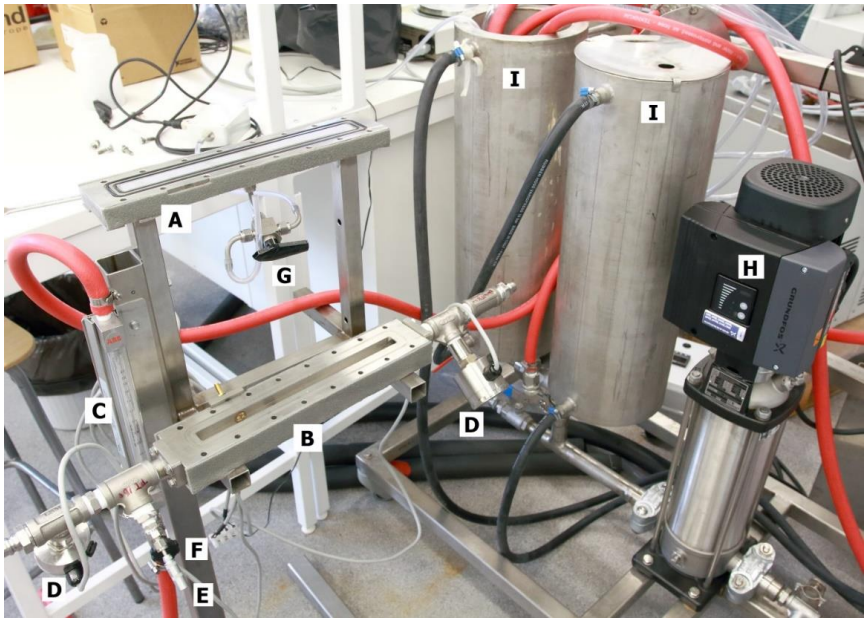

Figure 5. Filtration system equipped with the UTDR tool. The system consists of: (A) bottom part of the module (bottom plate), where the membrane is set on the porous support plate; (B) cover part of the module (top plate), which has ultrasonic sensors integrated inside; (C) flow meter; (D) pressure meters; (E) temperature meter; (F) valve for pressure and flow rate control; (G) permeate port and valve for the sample; (H) pump; (I) temperature-controlled feed vessels.

The permeate and retentate were recycled back to the temperature-controlled feed vessel (Figure 6). Temperature was measured after the membrane module, and the data was used to control the feed vessel temperature automatically. Pressure and flow were controlled with a valve after the filtration module and by changing the rotation speed of the pump. The volume of each feed vessel was 10 L. The maximum pressure applicable was 10 bar.

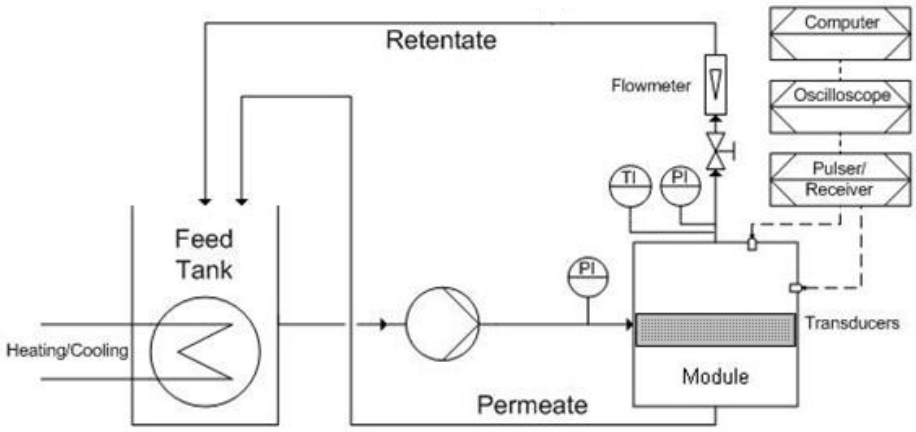

Figure 6. UTDR equipment connected to the crossflow filtration setup.

The stainless steel UF module consisted of a bottom and a cover part. The bottom part had a membrane sealing and porous support plate to enable permeate collection (Figure 7a). The cover part had a filtration channel, inlet, outlet and UTDR transducers (Figure 7b). The size of the filtration channel was 18 mm * 18 mm * 310 mm, and the membrane area was 55.8 cm^2.

a)

b)

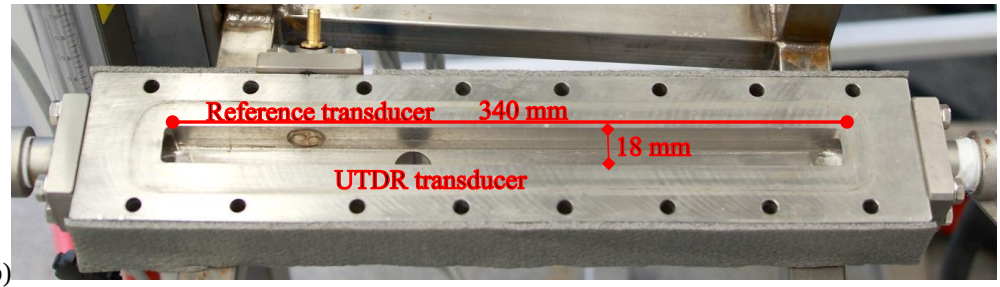

Figure 7. a) Bottom plate and b) top plate (upside down) of the UTDR module.

The ultrasonic transducers were integrated inside in the upper part of the membrane module (Figure 8). They were at the same level with the flow channel wall, so that they would not cause any extra turbulence in the module. One UTDR transducer was positioned sideways in the filtration channel for reference transducer measurement to determine sonic velocity, and one was on top of the cover part tangentially towards the membrane for time-of-flight measurement (Figures 7b and 8). The reference transducer was used to measure the time of flight of known distance. Thus, sonic velocity could be calculated by dividing the constant distance with the measured time of flight. The determined sonic velocity could be applied in Equation (1) (Chapter 8.1.1) to achieve environmental compensation (Publication I). Environmental compensation means that if the process conditions change during the filtration, the reference transducer measurements correct the sonic velocity in the UTDR measurements and thus improve its accuracy.

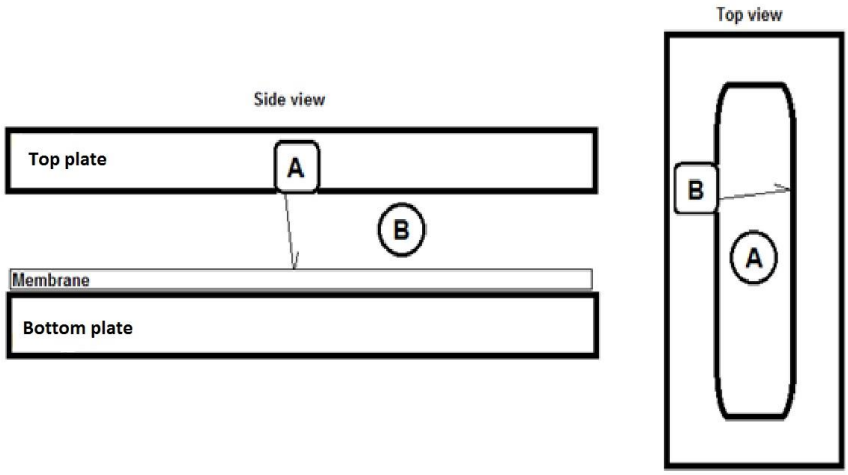

Figure 8. UTDR transducer configuration. Transducer A measures the time of flight to the membrane surface and transducer B measures the time of flight to the filtration channel wall whose distance is constant.

A cover part with a 1 mm high filtration channel was built to the module to be used with the double transducer (Figure 9). The size of the filtration channel of the second cover part was 1 mm * 18 mm * 310 mm and the membrane area was 55.8 cm^2. It was used in the inorganic fouling experiments with a double transducer presented in Publication II.

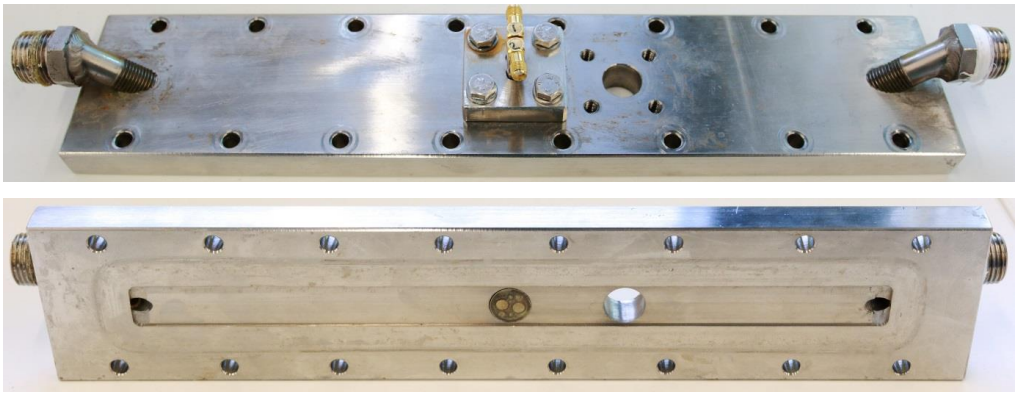

Figure 9. Cover part for the UTDR module with an only 1 mm high filtration channel and two positions for double transducers.

As can be seen in Figure 9, the feed channel was designed to be narrower to decrease the measurement distance of the UTDR transducer. A narrower channel also enhances shear rate over the membrane, which reduces fouling and represents better hydrodynamic properties of modules used in the industry. The reference transducer could not be positioned sideways in the 1 mm high channel as it was used in the module presented in Figure 7b, and thereby the reference measurement was achieved with a double transducer, where two transducers measured the same path from a different distance (Publication II).

Two different types of ultrasonic transducers were used during the study, a self-manufactured 10 MHz single element immersion transducer, and a later designed and self-manufactured 10 MHz double immersion transducer. The self-manufactured single and double transducers were made of stainless steel with O-ring sealing (Figure 10). The pulse was connected via 50 Ohm coaxial SMA-connectors to the piezoelectric crystal and a 50 Ohm resistor in the tip of the transducer. The crystals and resistors were coupled electrically parallel to decrease resonance damping time. The commercial name for the piezoelectric crystals used was Pz26 (Navy I) (Cited Ferroperm-piezo). These crystals have been designed for underwater applications and they are made of lead zirconate titanate. The crystal size is 5 mm and it has 10 MHz resonance frequency. The Q-factor is higher than 1000, which is a relatively high coupling factor compared to other crystals in this class. The high Q-factor means that the oscillation frequency has a narrow bandwidth and the damping factor is low compared to lower Q-factor crystals. The tip of the transducer was covered with epoxy to protect the crystals and resistors from the solution. Iron particles were mixed in the epoxy layer to enhance the adaption

of transducer vibration energy in water. No coupling agent was needed with the integrated sensors as they were immersed in water.

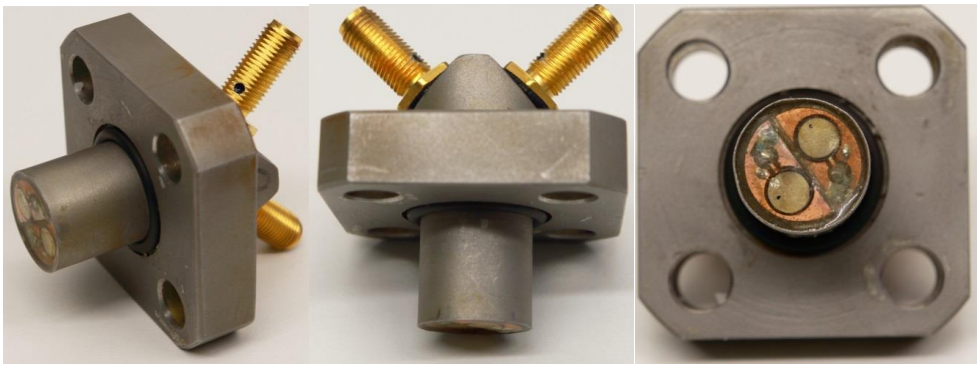

Figure 10. LUT-made double transducers. The single-element transducers are similar, except that they have only one connector and the single element is in the middle of the tip of the transducer.

The double transducer consisted of two piezoelectric crystals which were at different distances from the target surface (Figure 11). Both crystals were used simultaneously to determine sonic velocity while measuring the distance. The idea was similar to the reference transducer measurements, where one transducer measured sonic velocity while the other measured the distance to the target surface.

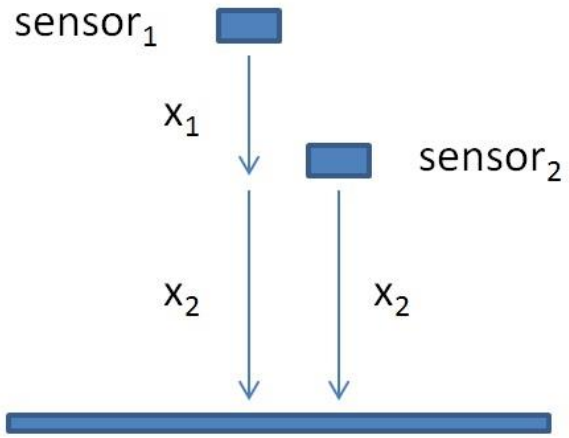

Figure 11. Principle of the double transducer. The fixed distance difference of the sensors to the target surface (x_1) can be used to determine sonic velocity.

The double transducer had to be calibrated before use to determine the fixed distance between the sensors. The calibration was done with a calibration platform designed and manufactured at LUT. The calibration platform (Figure 12) consists of an adjustable micrometre arm where the double transducer can be attached. An illustrative figure of the setup is shown in the Publication II (Figure 5).

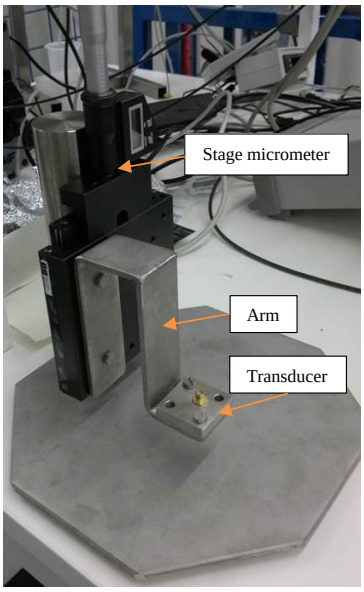

Figure 12. Calibration platform for double transducers.

In the calibration, the distance to the target surface can be changed by adjusting the arm with the micrometre. The arm with the transducer is placed in solution. Simultaneously, the times of both sensors are measured with an oscilloscope. From the results, it is possible to form linear regressions where the measured time is a function of distance (Figure 13).

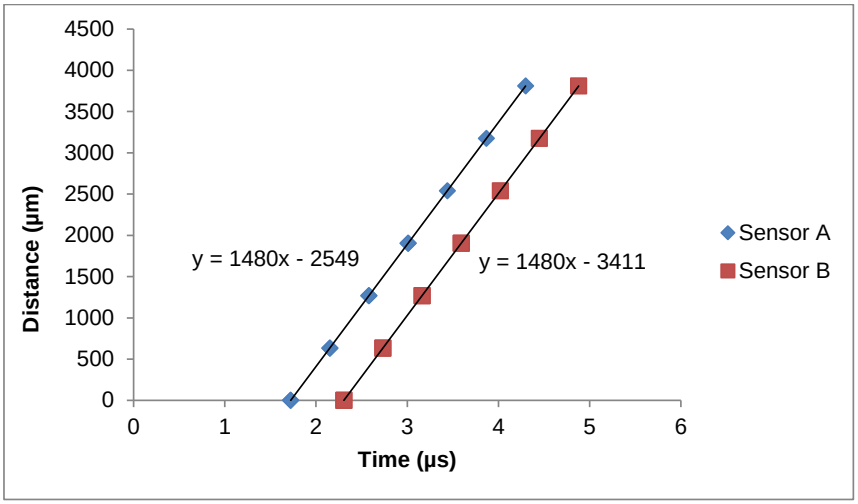

Figure 13. An example of calibration data. Sonic velocity and the distance between the sensors can be calculated from the equations in the figure.

As can be seen in Figure 13, the slope of the equation is the sonic velocity in the solution (1480 m/s). It is same in both equations, as both transducers are in the same solution. The distance difference between the transducer elements can be calculated from the difference between constant values in the equations: 3411 – 2549 = 862 (µm). This constant distance difference can be used to determine the sonic velocity when the double transducer is used in UTDR measurements.

A Tektronix 3052B oscilloscope was used in the experiments. It has 500 MHz bandwidth, 2 channels and 5 GS/s sample rate per channel. It was connected to a PC via the Ethernet. A LUT-manufactured pulser and amplifiers were used in all experiments.

9.3.2 Three-cell cross-flow filtration setup

A cross-flow filtration setup with three cells (Figure 14) was used in the experiments focused on measuring retention changes due to membrane compaction (Publications III and IV). The configuration of the filtration setup was similar to the filtration setup presented in Figure 6, except that there were three parallel membrane filtration cells. The dimensions of one filter cell were 1 mm * 20 mm * 230 mm, and the membrane area was 46 cm^2. The volume of the feed tank with pipe lines was 25 L.

Figure 14. Cross-flow filtration setup with three cells.

9.4 Analyses

The most important analysis techniques used in this study were measurement of the organic carbon content and examination of the membrane with a scanning electron microscope (SEM).

A Shimadzu Total Organic Carbon 5050A analyzer was used to analyze the amount of carbon in the samples. Two parallel samplings were used with <2 % deviation. The carbon content data of the feed solution and permeate was used to calculate the membrane PEG retention in the retention experiments (Publications III and IV).

A JEOL JSM-5800 Scanning Electron Microscope was used to analyze the possible changes in the membrane structure occurring due to compaction, and in the fouling experiments to detect inorganic fouling on the membrane surface. All membrane samples which required cross-sectional analysis were cut in liquid nitrogen to prevent the forming of cross-sectional structural changes in the membranes due to cutting. Freezing the sample in a water-ethanol (1:1) solution prevented the sample structure collapsing due to the pressure of cutting. The size of one sample was approximately 1 cm^2. The samples were coated with 2-20 nm thin gold

layers. 10 kV acceleration voltage and 10 mm working distance were the parameters used in the secondary electron imaging pictures.

9.5 Filtration experiments

The experiments can be divided into UTDR validation where the sensitivity of the UTDR signal and the accuracy of the system were tested, and into membrane compaction experiments.

9.5.1 Pre-treatment of the membranes

The membranes were pre-treated by soaking them in an alkaline water solution (pH=12) for 20 minutes to remove preservatives and to wet the membranes. Then the membranes were rinsed and stored with RO-treated water.

9.5.2 UTDR validation

The purpose of the experiments was to study how well the built UTDR setup with integrated transducers can detect fouling and what its accuracy and sensitivity are. The accuracy of the developed UTDR system with the reference transducer and double transducer was studied and presented in Publications I and II.

When the sensitivity of the UTDR system in the monitoring of inorganic fouling was evaluated, a $CaCO_3$ model solution was made by mixing $CaCl_2$ and $NaHCO_3$ solutions. A Desal 5 DK membrane was used in the experiments. The Langelier saturation index was used to estimate the supersaturation point of the solution. The pH of the solution was kept under the supersaturation point, so that the concentration where saturation occurs would only happen due to concentration polarization on the membrane surface and lead to fouling of the membrane and not of the whole filtration equipment. During the experiments, the dead-end filtration mode was used as in the Publication II. Flux, time- and amplitude-domain measurements were performed. After the experiments, SEM was used to confirm the state of the membrane surface.

9.5.3 Membrane compaction studies with the developed UTDR system

The purpose of the measurements was to link the membrane compaction to the membrane flux and retention changes. Modification of the pore sizes of the membranes with compaction in different temperatures was studied. Also reversible and irreversible compaction were measured and confirmed with real-time measurements. The experiments and results were explained in detail in Publications III and IV.

Compaction experiments were performed with RO-treated water in the filtration system with UTDR monitoring. Ultrafiltration membranes made by Microdyn-Nadir and Vladipor (Table IV) were used in the experiments. The temperature was held constant at 30, 50 or 70 °C, and the pressure was changed from 1 to 7 bar while the membrane thickness was monitored with the UTDR, and the flux was measured. Before and after the compaction measurement, the membrane distance values were read at 0.15 bar pressure, which was expected to cause no compaction. This 0.15 bar value in the beginning was set as a starting value before the compaction experiment to hold the membrane still against the support plate and to prevent it from floating. After the compaction experiment, when the reading was taken again at 0.15 bar, the value was the distance of how much the membrane recovered after the pressure was released. From this value, it is possible to calculate the reversible and irreversible compaction values by a simple subtraction when the starting value is known. Scanning Electron Microscope (SEM) images were taken after the compaction experiments to analyze the irreversible compaction of the membranes.

The influence of compaction on the retention of the membranes was examined by using the three-cell filtration setup. PEG 6000 was used for the 20 kDa and PEG 8000 for the 30 kDa MWCO membranes. The retention of the membranes was determined before and after compaction as a function of flux through the membrane. The retention samples were analyzed with TOC.

10 RESULTS AND DISCUSSION

10.1 Validation of the UTDR equipment

UTDR time-domain accuracy with the reference transducer was tested with constant condition experiments. In Publication I, the accuracy of the system was tested with temperature varying between 25-60 °C at different pressures. Amplitude-domain sensitivity was tested with inorganic fouling experiments. The results were compared with results presented in the literature. However, it was often not possible to compare the results directly, as the monitoring and filtration setup, filtration conditions, and foulants or the morphology of the foulants were different.

10.1.1 Time-domain accuracy of the UTDR setup with a reference transducer

The purpose of these experiments was to determine the measurement accuracy of the UTDR setup with a reference transducer. The distance to the aluminium surface was measured in constant conditions. The foil was used to avoid error coming from the compaction of the polymeric membrane. The duration of one experiment was 16 minutes, and the distance was measured 16 times to calculate standard deviation for the measurements. The test was repeated 5 times. Experimental data from one accuracy test is shown in Figure 15.

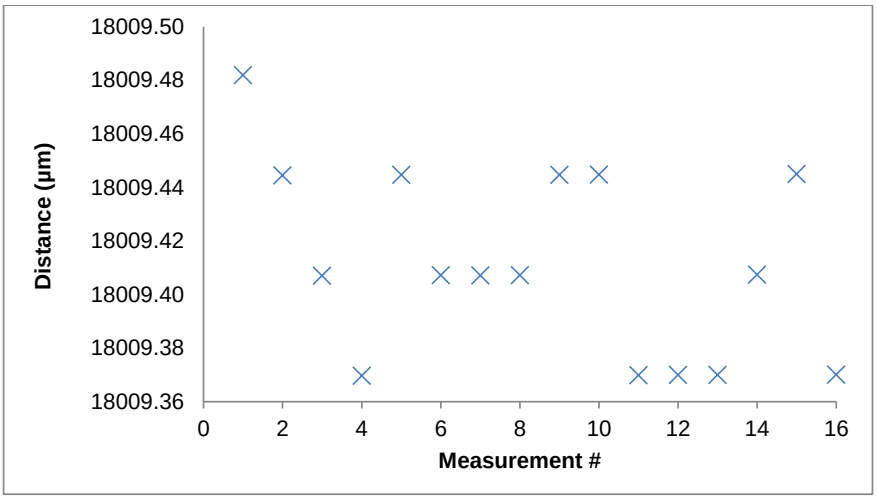

Figure 15. Experimental data of one measurement accuracy test of the UTDR setup with a reference transducer. The ~18000 µm distance to the aluminum surface was measured 16 times during 16 minutes in constant conditions.

As can be seen in the experimental data presented in Figure 15, the distance measurement varied from 18009.36 to 18009.48 µm, with standard deviation of 0.0358 µm for 16 measurements. With five repeated experiments, the measurement accuracy of the UTDR setup with a reference transducer was determined to be 0.042 µm. However, this accuracy represents only how accurate measurements can be done with this UTDR setup in constant conditions. The measurement accuracy decreases in real filtration conditions which are not as stable as those in this experiment. Changing filtration conditions affect sonic velocity, which affects the measurement accuracy due to the fact that sonic velocity is different between the sonic wave path of the UTDR transducer and the sonic wave path of the reference transducer.

Typical filtration conditions affecting sonic velocity are the temperature, pressure and concentration of the medium where the sound travels. Pressure is known to have a minor impact on the sonic velocity of fluids, as they are almost incompressible. However, especially temperature has a relatively great effect on sonic velocity and thus on the measurement accuracy of UTDR. Without a reference transducer, the accuracy of UTDR decreases dramatically in conditions where the temperature varies (Figure 16).

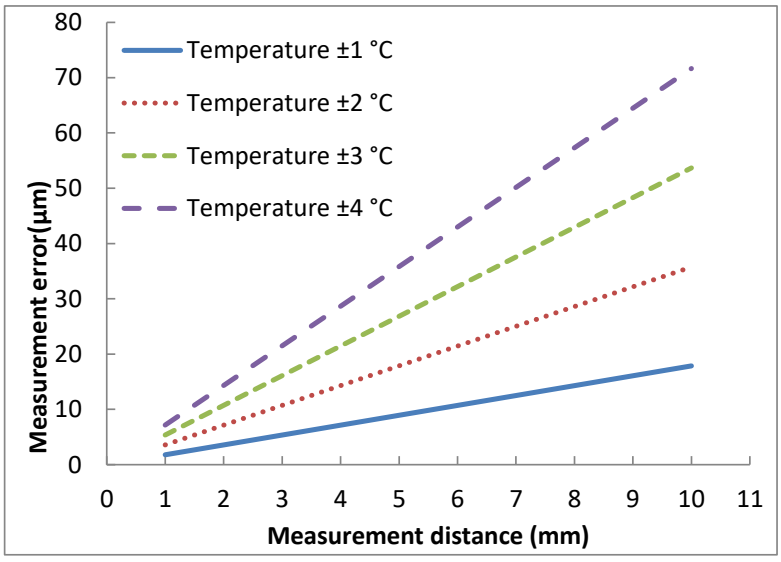

Figure 16. UTDR measurement error for pure water, caused by temperature change as a function of measurement distance. The error has been calculated by using an experimental model for sound velocity presented by Belogol'skii et al. (1999). The use of the model is explained in depth in Publication I.

As can be seen in Figure 16, the measurement error is directly proportional to the measurement distance. Although the UTDR measurement accuracy has been reported by Peterson et al. (1998) to be 0.75 µm with a configuration where there is no reference transducer and constant filtration conditions, the varying temperature may easily cause higher uncertainty in the measurements. For example, if the temperature varies by ±1 °C and the measurement distance is 5 mm (filtration channel height), the measurement error can be as high as 9 µm (Figure 16).

In non-constant conditions, without a reference transducer, the measurement error would be so significant that UTDR measurement would be practically useless. The accuracy of the UTDR setup with a reference transducer was determined in Publication I. In non-constant conditions, the measurement accuracy varied between 0.6-2.0 µm when the temperature was changed from 25 to 60 °C at the pressures of 0.1, 0.3 and 0.5 MPa. Such accuracy in non-constant filtration conditions is similar to that reported by Peterson et al. (1998) in constant filtration conditions (0.75 µm), which proves the functionality of the UTDR setup with a reference transducer.

In summary, the measurement accuracy of the UTDR setup can be improved with a reference transducer which is used to determine sonic velocity simultaneously with UTDR measurements. Without the determination of sonic velocity, the UTDR measurements are sensitive to measurement errors from temperature and concentration changes.

10.1.2 Amplitude-domain sensitivity to detect inorganic fouling with transducers integrated inside the module

The purpose of these experiments was to test the sensitivity of UTDR to detect inorganic fouling with UTDR transducers integrated inside the module as amplitude domain. In the literature, transducers have been used to monitor fouling through the top plate of the module or under the membrane. Positioning the transducer near the membrane surface inside the module was expected to have better sensitivity for detection, as in that case the measurement distance decreases and the sound does not have to penetrate the top plate of the module or the membrane.

The inorganic fouling experiment results of this study showed clearly that the UTDR system with transducers integrated inside the module was more sensitive to detect $CaCO_3$ fouling (Figures 17a and b) than what had been earlier reported by Mizrahi et al. (2012) (Figure 18) when the fouling was detected through the top plate of the module.

a) 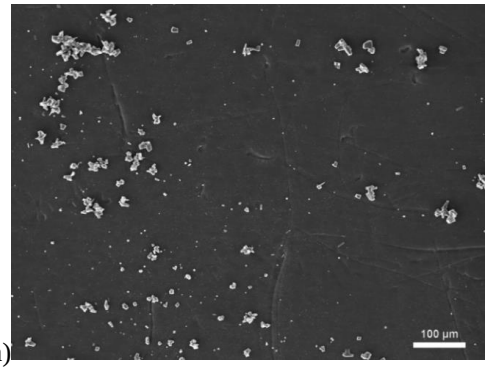

b) 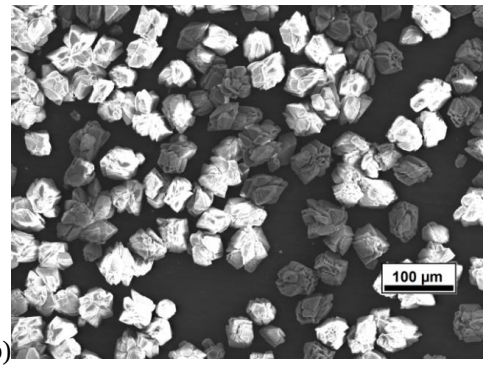

Figure 17. $CaCO_3$ fouling detection with UTDR transducers integrated inside the module. Signal amplitude change was a) 8 % and b) 49 %.

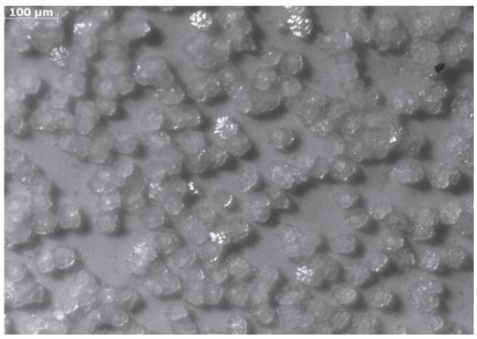

Figure 18. Reference results for the inorganic fouling test (Figure 17a and b), published by Mizrahi et al. (2012). The signal amplitude change was 2.6 %. The average crystal size was 50 µm and the area of coverage was 51 %.

As can be seen in Figures 17a and b, the sensitivity of UTDR to detect $CaCO_3$ fouling as a percentage change of signal amplitude was better than that reported by Mizrahi et al. (2012) (Figure 18). The CaCO3 fouling layer in figures 17b and 18 has similar size of crystals and coverage, but the amplitude changes with the transducer integrated inside the module was 49 %, whereas the changes measured through the top plate were only 2.6 %. The better sensitivity to detect fouling was expected to be due to the transducer which was integrated inside the membrane module, because when measured through the top plate, the plate will attenuate and scatter some of the signal energy, which will decrease the sensitivity of the measuring system to detect the changes. The transducer frequency was the same in both studies, 10 MHz, and the results are thus comparable. Frequency affects the penetration of the signal and sensitivity to detect the changes.

R. Sanderson et al. (2002) observed that the thickness of the $CaCO_3$ fouling/crystal layer affected the amplitude of the UTDR signal. In their study the calcite layer formed a new peak, which indicates that the thickness of the fouling layer was thicker than the one observed in the present study where the signal from the membrane surface was only enhanced. If the thickness of the inorganic layer is greater than the spatial resolution of the ultrasonic signal, a new peak will be formed in the reflected echo. If the thickness of the inorganic layer is less than the spatial resolution, the reflected energy will sum up with the peak from the next interface enhancing it.

Particle size and shape affect the UTDR signal amplitudes from the membrane surface, and that is why the UTDR amplitude values should be considered as indicative only. In the fouling experimens, $CaCO_3$ produced mainly hexagonal calcite crystals which enhanced the sound wave from the beginning of the crystal growth till the full fouling layer growth. Mairal et al. (2000) made a slightly different observation. $CaSO_4$ tends to grow a different kind of crystal structure than $CaCO_3$ fouling. In their studies, $CaSO_4$ fouling produced first spiky rosette structures which scattered the signal attenuating amplitudes of the reflected echo until the layer was thick enough to cover the membrane surface fully, and it formed a flat fouling layer enhancing the amplitudes. A scattered signal which attenuates the reflected echo may be misinterpreted as surface cleaning or organic fouling. Thus it is important to understand the ongoing fouling structure and the physical properties when the amplitude domain is used as the fouling monitoring method.

Li J. et al. (2007) also studied $CaCO_3$ fouling with a 10 MHz transducer. In their study $CaCO_3$ fouling also formed a new peak in front of the membrane reflection, and it also enhanced the membrane reflection, which was clearly seen in the differential signal. Li J. et al. (ibid.) report that a higher concentration produced a thicker and denser fouling layer structure. The denser structure of the fouling layer reflects the sound wave better, which is a similar effect as that observed with increasing fouling layer coverage on the membrane surface or membrane compaction. Thus, the amplitude method as fouling monitoring may be problematic to use when membrane compaction, fouling layer compaction and growth affect the amplitudes of the reflected echo and may be mixed up. The fouling layer reported by Li J. et al. (ibid.) had also vaterite and aragonite crystals whose shape and sound reflection properties are different from calcite crystals. Therefore, the sensitivity of fouling detection of the UTDR setups cannot be directly compared to the results presented by Li J. et al.

As a summary, transducers integrated inside the membrane module were more sensitive to detect inorganic fouling as the amplitude-domain method than measuring through the top plate of the module. However, the use of UTDR amplitude domain as a quantitative method is complicated. It requires good understanding of the ongoing fouling process and the physical properties of the monitored surfaces, or there will be a risk of misinformation.

10.2 Membrane compaction evaluation with the developed UTDR system

The purpose of these experiments was to study membrane compaction phenomena with the developed UTDR setup. Reversible and irreversible compaction was the topic of Publication III, and the link between flux, retention and membrane compaction was studied in Publication IV.

It was possible to detect the reversible and irreversible compaction of the membranes via time-domain measurements (Figures 19a-b). After the compaction experiment, when the pressure was released, the membranes recovered from the compaction, and this is called reversible compaction (elasticity). The viscoelastic compaction of the membrane, irreversible compaction, is the value that is left after the recoverable part. Both these compactions, reversible and irreversible compaction, affect the permeability of the membrane by decreasing it. The permeability decrease by reversible compaction can be mixed up with concentration polarization, as both of these effects are driving force (pressure) -dependent. This may lead to unnecessary process condition changes.

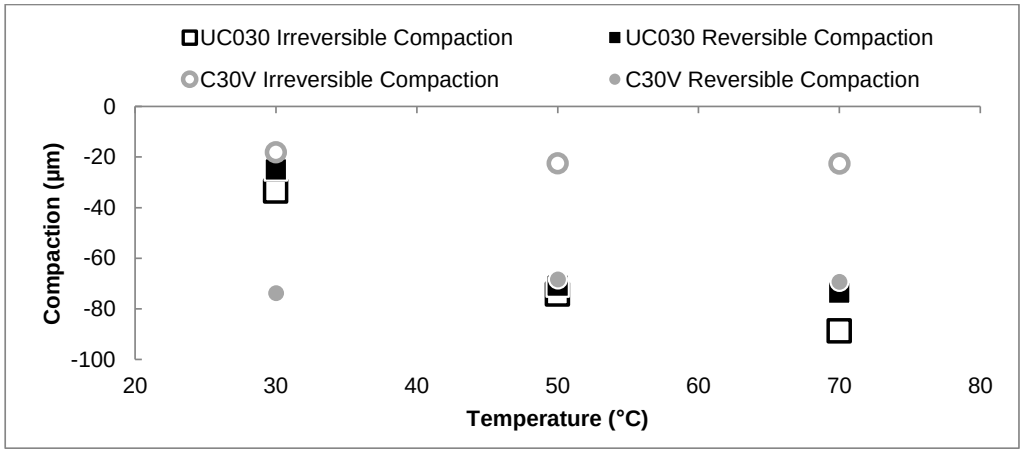

Figure 19a. Average irreversible and reversible compaction of three measurements of UC030 and the C30V membranes, after pressure was released from 7 bars at 30, 50 and 70 °C. The total thickness of the UC030 membrane was 265±5 µm and the one of C30V was 220±5 µm in the beginning of the test. (Publication IV)

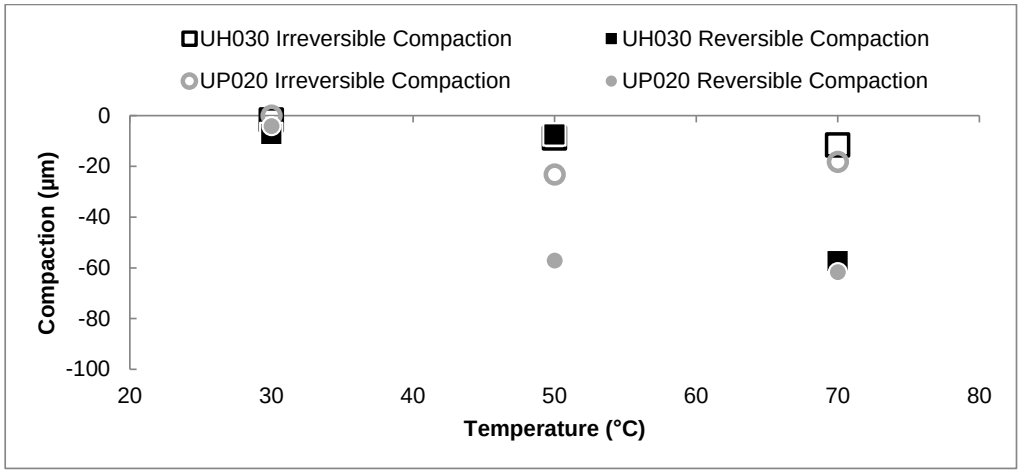

Figure 19b. Average irreversible and reversible compaction of three measurements of UH030 and UP020 membranes, after pressure was released from 7 bars at 30, 50 and 70 °C. The total thickness of the UH030 membrane was 225±5 µm and that of UP020 238±5 µm in the beginning of the test. (Publication IV)

As can be seen in Figures 19a-b, all the tested membranes had reversible and irreversible compaction. The regenerated cellulose membranes (UC030 and C30V) seem to be softer than the PES membranes (UP020 and UH030), which can be explained by the different membrane material. The measured compaction is the sum of the compaction of the backing, support and skin layer of the membrane. The skin layer of the membrane is usually only few nanometres thick, and that is why it is not measurable within the resolution of UTDR.

It could be noted on the basis of the experiments that the membrane structure influenced its compaction tendency. The membranes containing a macrovoid layer beneath the skin layer were more susceptible to compact than the membranes with a tighter structure supporting the layer under the skin. Kallioinen (2008) observed a similar phenomenon with membranes made from regenerated cellulose. The PES membranes used in the present study had no macrovoids straight beneath the skin layer, and there was no evidence of collapsed macrovoids (Publications III and IV). PES as the membrane material was also more compaction-resistant than the regenerated cellulose, which compacted remarkably more in all the tested pressures and temperatures. The observations made from the membrane structure changes due to compaction (Figures 20a-b) (Publications III-IV) were in good agreement with membrane compaction studies published earlier (Jönsson and Trägård 1990, Persson et al. 1995, Kallioinen 2008).

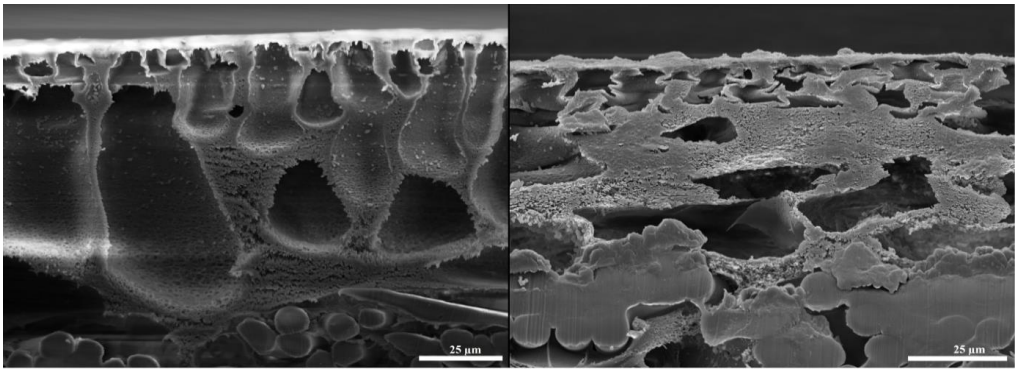

Figure 20a. The UC030 membrane before (left) and after (right) exposure to 7 bar and 70 °C conditions. Collapsed macrovoids can be seen beneath the skin layer. (Publication IV)

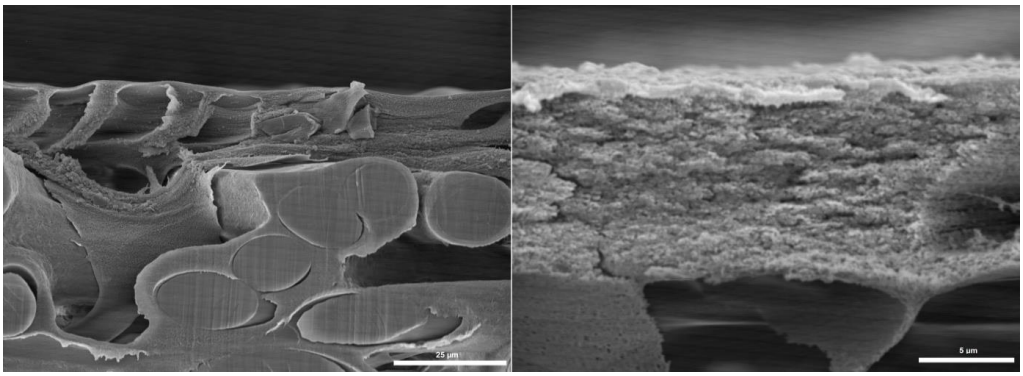

Figure 20b. Left: cross-section of a virgin C30V membrane before compaction; Right: detached support and skin layers of the C30V membrane after exposure to 7 bar and 70 °C conditions. (Publication IV)

As can be seen in Figure 20a, macrovoids right under the skin layer of the UC030 membrane tended to collapse. The denser structure of the C30V membrane resisted irreversible compaction better and was more elastic (Figures 19a and 20b). The UC030 membrane had a thicker support layer between the backing layer and the skin layer, which were more sensitive to irreversible compaction due to the high amount of macrovoids. After the structure had collapsed, it did not recover, and loss of permeability was inevitable due to increased hydrodynamic resistance from the densified support layer, in addition to the possible densification of the skin layer.

Membrane compaction in different pressures and temperatures was monitored to find out how increased temperature may affect the membrane compaction tendency in real time (Publications III and IV). The membrane compaction values in different pressures and temperatures are presented in Figures 21a-d.

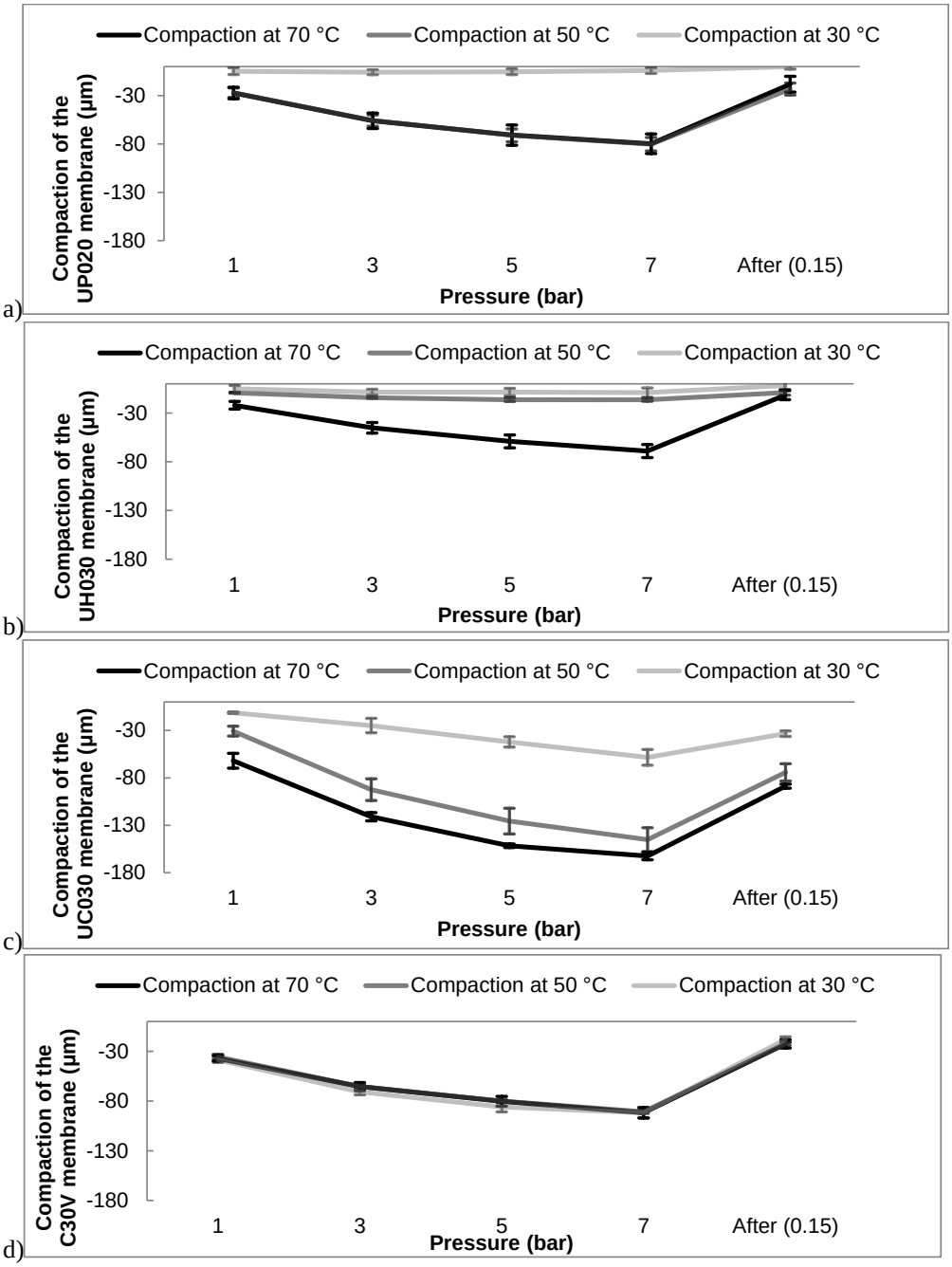

Figure 21. Compaction results of a) UP020, b) UH030, c) UC030, d) C30V membranes. The "Afrer (0.15)" value is the irreversible compaction value of the membranes. (Publication IV)

As can be seen in Figures 21a-d, compaction increased with increasing pressure and temperature in most cases. Exceptions were the PES membranes UP020 at 30 °C and UH030

at 30 and 50 °C, where compaction was independent of the pressure. At the temperature of 70 °C, the compaction of the UH030 membrane, and at 50 °C the compaction of the UP020 membrane increased significantly. However, most of that compaction was reversible, and higher pressure and temperature would be needed for increased irreversible compaction. The PES membranes had higher resistance against compaction than the RC membranes.

The compaction of the regenerated cellulose membranes was proportional to the filtration pressure at every temperature (Figures 21a-d). The glass transition temperature of dehydrated cellulose (84 °C, Roig et al. 2011) is lower than that of PES (230 °C, Ren et al. 2011), which partly explains its higher compaction. RC membranes are more hydrophilic than PES membranes. Water is hydrogen-bonded to the polar sites of cellulose macromolecules and works as a plasticizer, which decreases the glass transition temperature of the cellulose (Roig et al. 2011) and the mechanical stability of the membrane. Surprisingly, C30V was not as temperature-dependent as the other regenerated cellulose membrane UC030. The compaction of C30V was nearly the same at the temperatures of 30, 50 and 70 °C. This can be partially explained by the structure of the support layer, as shown above in Figures 20 a-b. The support layer of C30V was denser than and not as thick as the support layer of UC030. The structure of the support layer of C30V contained no macrovoids, which could explain the elastic behaviour of the structure. The thin and dense structure could recover better from the compaction than looser structure observed in the UC030 membrane. When there is less free space in the membrane structure (no macrovoids), the macromolecular rearrangement of the polymeric material is more limited. The force of the compression is more evenly distributed across the polymeric chains of the membrane, and thus it can recover better from it.

The membrane PEG retentions were studied before and after 15 h compaction at 7 bar pressure (Publication IV). Retention changes were assumed to be caused by the changes in the state of the skin layer. In the beginning, the retentions were measured at 0.5, 1.0 and 1.5 bar pressure. After the compaction, the retentions were measured at the same permeate fluxes as before the compaction. This was done because the permeate flux affects the retention. Practically, after the compaction a higher pressure was required to achieve the same permeate flux, as the compaction densifies the membrane and thus increases its hydrodynamic resistance, decreasing the permeability. Retention results before and after compaction at 50 °C are shown in Figure 22.

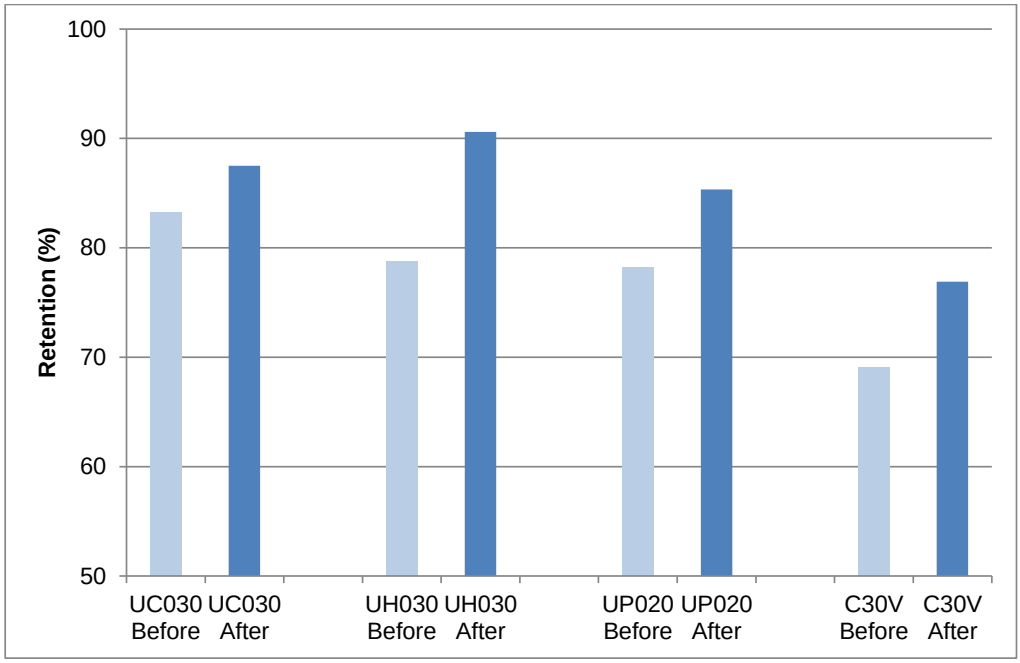

Figure 22. PEG retention results of tested membranes after 7 bar compaction at 50 °C. PEG 8 kg/mol was used in all other experiments except with the UP020 membrane, where PEG 6 kg/mol was used. The retentions were measured at 200 L/(m^2h) flux. (Publication IV)

As can be seen in Figure 22, the retentions tended to increase after the compaction, despite the membrane material or structural differences. Logically, the increased retention is due to membrane densification by compaction, which also affects the pore size and pore geometry. The relationship between membrane densification and pore size have been discussed by M. Mulder (1991). In most cases, the highest retentions were achieved after compaction at the temperature of 70 °C. A higher temperature softens the polymeric membrane material, as the thermal movement of water and polymeric molecules increases and thus the material compacts even more.

The UH030 membrane (Figure 22) had the highest retention inrease after compaction at 50 °C. The compaction data of the UH030 membrane (Figures 19b and 21b) showed that there occurred almost no compaction, but the retention changes were remarkable (Figure 22). Logically, the pore size of the skin layer had changed even thought the total thickness of the membrane was not changed. This leads to the understanding that the total thickness changes of

the whole membrane do not always present the retention changes or changes in the membrane skin layer.

The PEG retention of the C30V membrane decreased greatly in higher fluxes (Figure 23). Retention of above 70 % was achievable when the flux was 180 (L/(m^2h)), but when the pressure was increased so that the fluxes were near 620 (L/(m2h)), the retention decreased almost to zero. The low retention can be explained by the increase of concentration polarization at a high flux. As a phenomenon, this kind of change in membrane retention is interesting, as it is possible to modify the retention with the flux. Similarly, it was possible to modify the retention by nearly 10 %-units with compaction.

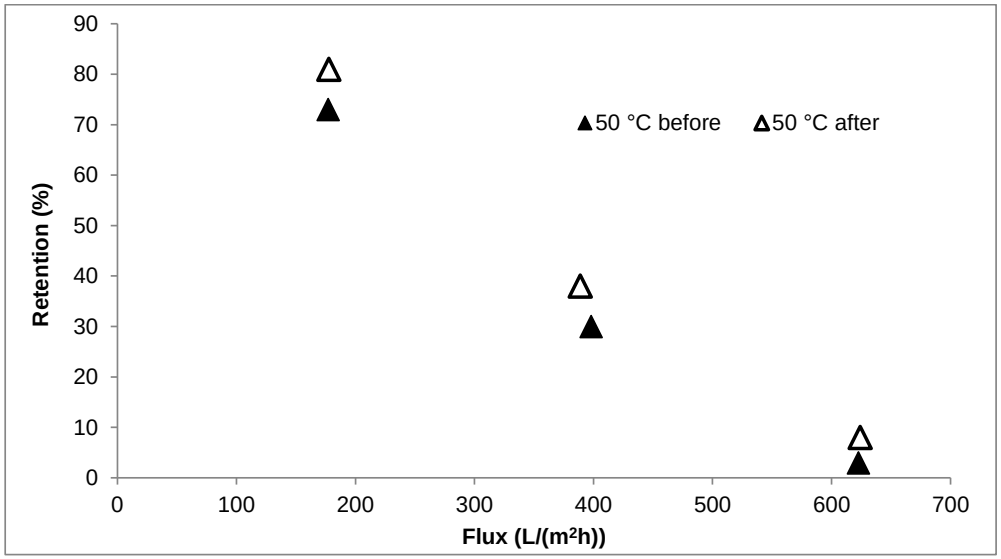

Figure 23. PEG retention results of the C30V membrane before and after 7 bar compaction at 50 °C. PEG 8 kg/mol was used as the model compound. Retentions were measured at 30 °C.

11 CONCLUSIONS

This thesis focused on improving an already existing UTDR measurement system with an additional reference transducer (Publication I) and a double transducer (Publication II). The developed UTDR measurement system with a reference transducer was validated in both time- and amplitude-domain modes. The time-domain measurements were made to validate the accuracy of the UTDR equipment in constant and changing filtration conditions. The sensitivity of the amplitude-domain method to detect inorganic fouling by using transducers integrated inside the membrane module was validated. After the validation of the UTDR measurement system with a reference transducer, it was utilised for membrane compaction studies. The studies focused on determining the reversible and irreversible compaction of the membrane, and on how they may affect the retention and permeability of RC and PES membranes at different temperatures (Publications III and IV).

With the reference transducer and the double transducer, it was possible to determine the sonic velocity during the UTDR measurements in real time. It was shown that the measured sonic velocity with the reference transducer made it possible to calculate the UTDR distance to the target surface more accurately than by using a constant sonic velocity value. If sonic velocity is assumed to be constant, the filtration conditions must be kept constant as well. In practical use, the filtration conditions may not be constant, which has limited the use of UTDR in industrial applications. A change of even one Celsius degree in the temperature may reduce the measurement accuracy of UTDR dramatically, and the error increases when the measurement distance increases. The use of a reference or a double transducer allows the filtration conditions to change without any limits to or effect on the accuracy of UTDR.

Higher measurement sensitivity to detect inorganic fouling compared to what has been presented in the literature was achieved. Transducers integrated inside the membrane module were more sensitive to detect $CaCO_3$ fouling than reported earlier, when fouling was measured through the top plate of the module. This was expected to be due to the fact that measurement through the top plate of the module scatters and attenuates the signal, resulting in a decrease in the sensitivity of UTDR. Also, the ultrasonic signal attenuates less when the distance between the transducer and the membrane surface decreases.

UTDR with a reference transducer was used to measure the reversible and irreversible compaction of the membranes in real time. Both the membrane structure and the material

affected the compaction tendency of RC and PES membranes. Macrovoids in the support layer weaken the structure of the membrane and may lead to irreversible compaction when the macrovoids collapse. The PES membranes were mechanically stronger than the RC membranes, which could be explained by the higher glass transition temperature of the PES material and the higher hydrophilicity of the RC material. Water works as plasticizer with polymeric materials, and the higher hydrophilicity of the membrane material increases its extent.

The compaction data was linked with the retention results, which showed that the measured compaction was the total compaction of the membrane and it did not represent the state of the skin layer of the membrane, which had the biggest impact on the filtration properties. Compaction, reversible and irreversible, tended to increase with temperature in most cases, leading to a decrease in membrane permeability. Without knowing the effect of reversible compaction on membrane performance, it could be interpreted as concentration polarization. This may lead to the adoption of inappropriate mitigation methods. Also, by using non-optimal pre-compaction conditions, it is possible to lose membrane permeability by irreversible compaction. However, with right pre-compaction conditions it is possible to increase membrane retention and thus affect the overall separation process beneficially. To sum up, membrane compaction can be used to increase membrane retention to some extent, with the cost of permeability.

REFERENCES

Adikane, H.V., Nene, S.N., Kulkarni, S.S., Baxi, P.U., Khatpe, D.S., Aphale, P.A., 1997. Concentration of foot-and-mouth disease virus by ultrafiltration. *J. Membr. Sci.*, 132, 91-96.

Aerts, P., Greenberg, A.R., Leysen, R., Krantz, W.B., Reinsch, V.E., Jacobs, P.A., 2001. The influence of filler concentration on the compaction and filtration properties of Zirfon®-composite ultrafiltration membranes. *Sep. Purif. Technol*., 22-23, 663-669.

Airey, D., Yao, S., Wu, J., Chen, V., Fane, A.G., Pope, J.M., 1998. An investigation of concentration polarization phenomena in membrane filtration of colloidal silica suspensions by NMR micro-imaging. *J. Membr. Sci.*, 145, 145-158.

AL-Hobaib, A.S., AL-Sheetan, Kh.M., El Mir, L., 2016. Effect of iron oxide nanoparticles on the performance of polyamide membrane for ground water purification. *Mat. Sci. Semicon. Proc*., 42, 107-110.

Altmann, J., Ripperger, S., 1997. Particle deposition and layer formation at the crossflow microfiltration. *J. Membr. Sci*., 124, 119-128.

Amirilargani, M., Sadrzadeh, M., Sudhölter, E.J.R., de Smet, L.C.P.M., 2016. Surface modification methods of organic solvent nanofiltration membranes. *Chem. Eng. J.*, 289, 562-582.

An, G., Lin, J., Li, J., Li, X., Jian, X., 2011. Non-invasive measurement of membrane scaling and cleaning in spiral-wound reverse osmosis modules by ultrasonic time-domain reflectometry with sound intensity calculation. *Desalionation*, 283, 3-9.

Arunkumar, A., Etzel, M.R., 2015. Negatively charged tangential flow ultrafiltration membranes for whey protein concentration. *J. Membr. Sci.*, 475, 340-348.

Bagci, P.O., 2014. Effective clarification of pomegranate juice: A comparative study of pretreatment methods and their influence on ultrafiltration flux. *J. Food. Eng.*, 141, 58-64.

Baker, R.W., 2005. *Membrane technology and applications*, 2nd Ed., John Wiley & Sons, Ltd., England.

Bannwarth, S., Darestani, M., Coster, H., Wessling, M., 2015. Characterization of hollow fiber membranes by impedance spectroscopy. *J. Membr. Sci.*, 473, 318-326.

Bartman, A.R., Lyster, E., Rallo, R., Christofides, P.D., Cohen, Y., 2011. Mineral scale monitoring for reverse osmosis desalination via real-time membrane surface image analysis. *Desalination*, 273, 64-71.

Bazzarelli, F., Piacentini, E., Poerio, T., Mazzei, R., Cassano, A., Giorno, L., 2016. Advances in membrane operations for water purification and biophenols recovery/valorization from OMWWs. *J. Membr. Sci.*, 497, 402-409.

Belogol'skii, V.A., Sekoyan, S.S., Samorukova, L.M., Stefanov, S.R., Levtsov, V.I., 1999. Pressure dependence of the sound velocity in distilled water. *Meas. Tech.*, 42, 406–413.

Benavente, J., 2009. Chapter 9: Electrical characterization of membranes. *Monitoring and visualizing membrane-based processes*. Edited by Güell et al., WILEY-VCH Verlag GmbH & Co. KGaA, Germany.

Bilad, M.R., Arafat, H.A., Vankelecom, I.F.J., 2014. Membrane technology in microalgae cultivation and harvesting: A review. *Biotechnol. Adv.*, 32, 1283-1300.

Böhm, L., Kraume, M., 2015. Fluid dynamics of bubble swarms rising in Newtonian and non-Newtonian liquids in flat sheet membrane systems. *J. Membr. Sci.*, 475, 533-544.

Bohonak, D.M., Zydney, A.L., 2005. Compaction and permeability effects with virus filtration membranes. *J. Membr. Sci*., 254, 71-79.

Bond, L.J., Greenberg, A.R., Mairal, A.P., Loest, G., Brewster, J.H., Krantz, W.B., 1995. Real-time nondestructive characterization of membrane compaction and fouling. *Quantitative Nondestructive Evaluation*, 14, 1167-1173.

Cao, X., Loussaert, J.A., Wen, Z-Q., 2016. Microspectroscopic investigation of the membrane clogging during the sterile filtration of the growth media for mammalian cell culture. *J. Pharmaceut. Biomed*., 119, 10-15.

Cen, J., Vukas, M., Barton, G., Kavanagh, J., Coster, H.G.L., 2015. Real time fouling monitoring with Electrical Impedance Spectroscopy. *J. Membr. Sci*., 484, 133-139.

Chai, G.-Y., Greenberg, A.R., Krantz, W.B., 2007. Ultrasound, gravimetric, and SEM studies of inorganic fouling in spiral-wound membrane modules. *Desalination*, 208, 277-293.

Chan, R., Chen, V., 2004. Characterization of protein fouling on membranes: opportunities and challenges. *J. Membr. Sci.*, 242, 169-188.

Chang, S., Yeo, A., Fane, A., Cholewa, M., Ping, Y., Moser, H., 2007. *J. Membr. Sci*., 304, 181-189.

Charcosset, C., Yousefian, F., Thovert, J.F., Adler, P.M., 2002. Calculation of flow and solute deposition through three-dimensional reconstructed model of microporous membranes. *Desalination*, 145, 133-138.

Chen, J., Huang, J.-Y., 2014. Texture analysis of UTDR images for enhancement of monitoring and diagnosis of membrane filtration. *Chemometr. Intell. Lab*., 138, 142-152.

Chen, J.C., Li, Q., Elimelech, M., 2004. In situ monitoring techniques for concentration polarization and fouling phenomena in membrane filtration. *Adv. Colloid. Interfac*., 107, 83-108.

Chen, V., Li, H., Fane, A.G., 2004. Non-invasive observation of synthetic membrane processes – a review of methods. *J. Membr. Sci.*, 241, 23-44.

Chilcott, T.C., Cen, J., Kavanagh, J.M., 2015. In situ characterization of compaction, ionic barrier and hydrodynamics of polyamide reverse osmosis membranes using electrical impedance spectroscopy. *J. Membr. Sci*., 477, 25-40.

Chimini, A., Moresi, M., 2016. Assessment of the optimal operating conditions for pale lager clarification using novel ceramic hollow-fiber membranes. *J. Food. Eng.*, 173, 132-142.

Chong, T.H., Wong, F.S., Fane, A.G., 2007. Fouling in reverse osmosis: Detection by non-invasive techniques. *Desalination*, 204, 148-154.

Cobry, K.D., Bright, V.M., Greenberg, A.R., 2011a. Integrated electrolytic sensors for monitoring of concentration polarization during nanofiltration. *Sensor. Actuat. B-Chem.*, 160, 730-739.

Cobry, K.D., Yuan, Z., Gilron, J., Bright, V.M., Krantz, W.B., Greenberg, A.R., 2011b. Comprehensive experimental studies of early-stage membrane scaling during nanofiltration. *Desalination*, 283, 40-51.

Coster, H.G.L., Chilcott, T.C., Coster, A.C.F., 1996. Impedance spectroscopy of interfaces, membranes and ultrastructures. *Bioelectroch. Bioener.*, 40, 79-98.

Coster, H.G.L., Kim, K.J., Dahlan, K., Smith, J.R., Fell, C.J.D., 1992. Characterisation of ultrafiltration membranes by impedance spectroscopy. I. Determination of the separate electrical parameters and porosity of the skin and sublayers. *J. Membr. Sci.*, 66, 19-26.

Crespo, J.P.S.G., Trotin, M., Hough, D., Howell, J.A., 1999. Use of fluorescence labelling to monitor protein fractionation byultrafiltration under controlled permeate flux. *J. Membr. Sci.*, 155, 209-230.

CSLM SP8 gSTED 3X Leica. University of Zurich. Available: http://www.zmb.uzh.ch/Instrumentation/LightMicroscopy/SuperResolution/gSTED3X.html (Cited: 17.6.2015)

Czekaj, P., López, F., Güell, C., 2000. Membrane fouling during microfiltration of fermented beverages. *J. Membr. Sci.*, 166, 199-212.

Dunkers, J.P., Cicerone, M.T., Washburn, N.R., 2003. Collinear optical coherence and confocal fluorescence microscopies for tissue engineering. *Opt. Express.*, 11, 3074-3079.

Ebert, K., Fritsch, D., Koll, J., Tjahjawiguna, C., 2004. Influence of inorganic fillers on the compaction behavior of porous polymer based membranes. *J. Membr. Sci*., 233, 71-78.

Feng, X., Guo, Y., Chen, X., Zhao, Y., Li, J., He, X., Chen, L., 2012. Membrane formation process and mechanism of PVDF-g-PNIPAAm thermo-sensitive membrane. *Desalination*, 290, 89-98.

Ferroperm-piezoceramics (formerly known as, Meggitt bought the company). Piezoceramic Components Production. Available online: http://www.meggittsensingsystems.com/ capabilities/piezoceramic-components-production.html (Cited: 25.6.2015).

Frank, A., Lipscomb, G.G., Dennis, M., 2000. Visualization of concentration fields in hemodialyzers by computer tomography. *J. Membr. Sci.*, 175, 239-251.

Frank, A., Lipscomb, G.G., Dennis, M., 2001. Visualizing the entrapment of air pockets in the shell of a hemodialyzer during wet-out. *Chem. Eng. Commun.*, 184, 139-155.

Fridjonsson, E.O., Vogt, S.J., Vrouwenvelder, J.S., Johns, M.L., 2015. Early non-destructive biofilm detection in spiral wound RO membranes using a mobile earth's field NMR. *J. Membr. Sci.*, 489, 227-236.

Fu, C., Cai, D., Hu, S., Miao, Q., Wang, Y., Qin, P., Wang, Z., Tan, T., 2016. Ethanol fermentation integrated with PDMS composite membrane: An effective process. *Bioresource Technol.*, 200, 648-657.

Gao, Y., Haavisto, S., Li, W., Tang, C.Y., Salmela, J., Fane, A.G., 2014. Novel approach to characterizing the growth of a fouling layer during membrane filtration via optical coherence tomography. *Environ. Sci. Technol.*, 48, 14273-14281.

Gaucher, C., Jaouen, P., Comiti, J., Legentilhomme, P., 2002a. Determination of cake thickness and porosity during cross-flow ultrafiltration on a plane ceramic membrane surface using and electrochemical method. *J. Membr. Sci.*, 210, 245-258.

Gaucher, C., Jaouen, P., Legentilhomme, P., Comiti, J., 2002b. Suction effect on the shear stress at a plane ultrafiltration ceramic membrane surface. *Sep. Sci. Technol.*, 37, 2251-2270.

Gaucher, C., Jaouen, P., Legentilhomme, P., Comiti, J., 2003. Influence of fluid distribution on the ultrafiltration performance of a ceramic flat sheet membrane. *Sep. Sci. Technol.*, 38, 1949-1962.

Gaucher, C., Legentilhomme, P., Jaouen, P., Comiti, J., 2002c. Influence of fluid distribution on the wall shear stress in a plane ultrafiltration module using an electrochemical method. *Trans. Inst. Chem. Eng.*, 80, 111-120.

Gaucher, C., Legentilhomme, P., Jaouen, P., Comiti, J., Pruvost, J., 2002d. Hydrodynamics study in a plane ultrafiltration module using an electrochemical method and particle image velocimetry visualization. *Exp. Fluids*, 32, 283-293.

Gésan, G., Daufin, G., Merin, U., 1995. Performance of whey crossflow microfiltration during transient and stationary operating conditions. *J. Membr. Sci.*, 104, 271-281.

Gladden, L.F., 1994. Nuclear magnetic resonance in chemical engineering: principles and applications. *Chem. Eng. Sci.*, 49, 3339-3408.

Goulas, A.K., Kapasakalidis, P.G., Sinclair, H.R., Rastall, R.A., Grandison, A.S., 2002. Purification of oligosaccharides by nanofiltration. *J. Membr. Sci.*, 209, 312-335.

Güell, C., Ferrando, M., López, F., 2009. *Monitoring and Visualizing Membrane-Based Processes*. WILEY-VCH Verlag GmbH & Co. KGaA, Germany.

Hassan, I.B., Lafforgue, C., Ayadi, A., Schmitz, P., 2014a. in situ 3D characterization of bidisperse cakes using confocal laser scanning microscopy. *J. Membr. Sci.*, 466, 103-113.

Hassan, I.B., Lafforgue, C., Ayadi, A., Schmitz, P., 2014b. In situ 3D characterization of monodispersed spherical particle deposition on microsieve using confocal laser scanning microscopy. *J. Membr. Sci.*, 454, 283-297.

Homaeigohar, S.S., Elbahri, M., 2012. Novel compaction resistant and ductile nanocomposite nanofibrous microfiltration membranes. *J. Colloid. Interf. Sci*., 372, 6-15.

Huang, S., Voutchkov, N., Jiang S.C., 2013. Investigation of environmental influences on membrane biofouling in a Southern California desalination pilot plant. *Desalination*, 319, 1-9

Jhaneri, J.H., Murthy, Z.V.P., 2016. A comprehensive review on anti-fouling nanocomposite membranes for pressure driven membrane separation processes. *Desalination*, 379, 137–154.

Jian, K., Pintauro, P.N., Ponangi, R., 1996. Separation of dilute organic/water mixtures with asymmetric poly(vinylidene fluoride) membranes. *J. Membr. Sci.*, 117, 117-133.

Jiraratananon, R., Chanachai, A., 1996. A study of fouling in the ultrafiltration of passion fruit juice. *J. Membr. Sci.*, 111, 39-48.

Jogdand, A., Chaudhuri, A., 2015. Modeling of concentration polarization and permeate flux variation in a roto-dynamic reverse osmosis filtration system. *Desalination*, 375, 54–70.

Jönsson, A.-S., Trägårdh, G., 1990. Ultrafiltration applications. *Desalination*, 77, 135-179.

Judd, S., 2003. Chapter 2: Membrane Technology. In book: *Membranes for industrial wastewater recovery and re-use*. Edited by Judd, S. and Jefferson, B. Elsevier Ltd, Oxford, UK.

Judd, S., 2006. Chapter 2.1.4.4: Concentration Polarization. In book: *The MBR Book: Principles and Applications of Membrane Bioreactors in Water and Wastewater Treatment*. Elsevier Ltd, Oxford, UK.

Kallioinen, M., 2008. Doctoral Thesis: *Regenerated Cellulose Ultrafiltration Membranes in the Treatment of Pulp and Paper Mill Process Water*. Lappeenranta University of Technology, Acta Universitatis Lappeenrantaensis, 307, Finland.

Kang, S.-T., Subramani, A., Hoek, E.M.V., Deshusses, M.A., Matsumoto, M.R., 2004. Direct observation of biofouling in cross-flow microfiltration: mechanisms of deposition and release. *J. Membr. Sci.*, 244, 151-165.

Karabelas, A.J., Kostoglou, M., Koutsou, C.P., 2015. Modeling of spiral wound membrane desalination modules and plants – review and research priorities. *Desalination*, 356, 165-186.

Karjalainen, A., 2010. Doctoral Thesis: *Online Ultrasound Measurements of Membrane Compaction*. Lappeenranta University of Technology, Acta Universitatis Lappeenrantaensis, 409, Finland.

Kennedy, M. D., Kamanyi, J., Salinaz Rodriquez, S. G., Lee, N. H., Schippers, J. C., Amy, G., 2008. Chapter 6: Water treatment by microfiltration and ultrafiltration. In book: *Advanced membrane technology and applications*. Edited by Li, N.N., Fane, A.G., Ho, W.S.W., Matsuura, T., John Wiley & Sons, Inc., USA.

Kong, S., Aucamp, J., Titchener-Hooker, N.J., 2010. Studies on membrane sterile filtration of plasmid DNA using an automated multiwell technique. *J. Membr. Sci.*, 353, 144-150.

Kong, X., Zhou, M.-Y., Lin, C.-E., Wang, J., Zhao, B., Wei, X.-Z., Zhu, B.-K., 2016. Polyamide/PVC based composite hollow fiber nanofiltration membranes: Effect of substrate on properties and performance. *J. Membr. Sci.*, 505, 231-240.

Kools, W.F.C., Konagurthu, S., Greenberg, A.R., Bond, L.J., Krantz, W.B., van den Boomgaard, T.H., Strathmann, H., 1998. Use of ultrasonic time-domain reflectometry for real-time measurement of thickness changes during evaporative casting of polymeric films. *J. Appl. Polym. Sci*, 69, 2013-2019.

L´Hostis, E., Deslouis, C., Tribollet, B., Festy, D., 1996. EHD and steady state measurements for characterization of transport properties in a gel layer. *Electrohim. Acta*, 41, 1393-1399.

Lawson, K.W., Hall, M.S., Lloyd, D.R., 1995. Compaction of microporous membranes used in membrane distillation. I. Effect on gas permeability. *J. Membr. Sci.*, 101, 99-108.

Li, H., Fane, A.G., Coster, H.G.L., Vigneswaran, S., 2000a. An assessment of depolarisation models of crossflow microfiltration by direct observation through the membrane. *J. Membr. Sci.*, 172, 135-147.

Li, H., Fane, A.G., 2000b. New insights into membrane operation revealed by direct observation through the membrane. *Membrane Technology*, 2000, 10-14.

Li, H., Fane, A.G., Coster, H.G.L., Vigneswaran, S., 1998. Direct observation of particle deposition on the membrane surface during crossflow microfiltration. *J. Membr. Sci.*, 149, 83-97.

Li, H., Fane, A.G., Coster, H.G.L., Vigneswaran, S., 2003. Observation of deposition and removal behaviour of submicron bacteria on the membrane surface during crossflow microfiltration. *J. Membr. Sci.*, 217, 29-41.

Li, J., Hallbauer, D.K., Sanderson, R.D., 2003. Direct monitoring of membrane fouling and cleaning during ultrafiltration using a non-invasive ultrasonic technique. *J. Membr. Sci.*, 215, 33-52.

Li, J., Koen, L.J., Hallbauer, D.K., Lorenzen, L., Sanderson, R.D., 2005. Interpretation of calcium sulfate deposition on reverse osmosis membranes using ultrasonic measurements and a simplified model. *Desalination*, 186, 227-241.

Li, J., Liu, J., Yang, T., Changfa, X., 2007. Quantitative study of the effect of electromagnetic field on scale deposition on nanofiltration membranes via UTDR. *Water research*, 41, 4595-4610.

Li, J., Sanderson, R.D., 2002c. In situ measurement of particle deposition and its removal in microfiltration by ultrasonic time-domain reflectometry. *Desalination*, 146, 169-175.

Li, J., Sanderson, R.D., Chai, G.Y., 2006. A focused ultrasonic sensor for in situ detection of protein fouling on tubular ultrafiltration membranes. *SENSOR ACTUAT B-CHEM.*, 114, 182-191.

Li, J., Sanderson, R.D., Chai, G.Y., Hallbauer, D.K., 2005. Development of an ultrasonic technique for in situ investigating the properties of deposited protein during crossflow ultrafiltration. *J. Colloid Interface Sci.*, 284, 228-238.

Li, J., Sanderson, R.D., Hallbauer, D.K., Hallbauer-Zadorozhnaya, V.Y., 2002a. Measurement and modelling of organic fouling deposition in ultrafiltration by ultrasonic transfer signals and reflections. *Desalination*, 146, 177-185.

Li, J., Sanderson, R.D., Jacobs, E.P., 2002b. Non-invasive visualization of the fouling of microfiltration membranes by ultrasonic time-domain reflectometry. *J. Membr. Sci.*, 201, 17-29.

Li, X., Li, J., Wang, J., Wang, H., Cui, C., He, B., Zhang, H., 2014a. Direct monitoring of sub-critical flux fouling in a horizontal double-end submerged hollow fiber membrane module using ultrasonic time domain reflectometry. *J. Membr. Sci.*, 451, 226-233.

Li, X., Li, J., Wang, J., Wang, H., He, B., Zhang, H., 2013. Ultrasonic visualization of sub-critical flux fouling in the double-end submerged hollow fiber membrane module. *J. Membr. Sci.*, 444, 394-401.

Li, X., Li, J., Wang, J., Wang, H., He, B., Zhang, H., Guo, W., Ngo, H.H., 2014b. Experimental investigation of local flux distribution and fouling behavior in double-end and dead-end submerged hollow fiber membrane modules. *J. Membr. Sci.*, 453, 18-26.

Li, X., Li, J., Wang, J., Zhang, H., Pan, Y., 2012. In situ investigation of fouling behavior in submerged hollow fiber membrane module under sub-critical flux operation via ultrasonic time domain reflectometry. *J. Membr. Sci.*, 411-412, 137-145.

Li, X., Zhang, H., Hou, Y., Gao, Y., Li, J., Guo, W., Ngo, H.H., 2015. In situ investigation of combined organic and colloidal fouling for nanofiltration membrane using ultrasonic time domain reflectometry. *Desalination*, 362, 43-51.

Lin, Y.-H., Tung, K.-L., Wang, S.-H., Zhou, Q., Shung, K.K., 2013. Distribution and deposition of organic fouling on the microfiltration membrane evaluated by high-frequency ultrasound. *J. Membr. Sci.*, 433, 100-111.

Liu, J., Li, J., Chen, X., Zhang, Y., 2006. Monitoring of polymeric membrane fouling in hollow fiber module using ultrasonic nondestructive testing. *Trans. Nonferrous Met. Soc. China*, 16, 845-848.

Lu, W.-M., Tung, K.-L., Pan, C.-H., Hwang, K.-J., 2002. Crossflow microfiltration of moni-dispersed deformable particle suspension. *J. Membr. Sci.*, 198, 225-243.

Lu, X., Kujundzic, E., Mizrahi, G., Wang, J., Cobry, K., Peterson, M., Gilron, J., Greenberg, A.R., 2012. Ultrasonic sensor control of flow reversal in RO desalination – Part 1: Mitigation of calcium sulfate scaling. *J. Membr. Sci.*, 419-420, 20-32.

Lynnworth, L.C., 1989. *Ultrasonic measurements for process control-theory. Techniques, Applications*. Academic press, USA.

Mairal, A.P., Greenberg, A.R., Krantz, W.B., 2000. Investigation of membrane fouling and cleaning using ultrasonic time-domain reflectometry. *Desalination*, 130, 45-60.

Mairal, A.P., Greenberg, A.R., Krantz, W.B., Bond, L.J., 1999. Real-time measurement of inorganic fouling of RO desalination membranes using ultrasonic time-domain reflectometry. *J. Membr. Sci*., 159, 185-196.

Mänttäri, M., 1999. Doctoral Thesis: *Fouling management and retention in nanofiltration of integrated paper mill effluents*. Lappeenranta University of Technology, Acta Universitatis Lappeenrantaensis, 78, Finland.

Marselina, Y., Le-Clech, P., Stuetz, R., Chen, V., 2008. Detailed characterisation of fouling deposition and removal on a hollow fibre membrane by direct observation technique. *Desalination*, 231, 3-11.

Marselina, Y., Le-Clech, P., Stuetz, R.M., Chen, V., 2009. Chapter 14: Towards Fouling Monitoring and Visualization in Membrane Bioreactors. *Monitoring and visualizing membrane-based processes*. Edited by Güell et al., WILEY-VCH Verlag GmbH & Co. KGaA, Germany.

McDonogh, R.M., Bauser, H., Stroh, N., Chmiel, H., 1990. Concentration polarisation and adsorption effects in cross-flow ultrafiltration of proteins. *Desalination*, 79, 217-231.

McDonogh, R.M., Bauser, H., Stroh, N., Chmiel, H., 1992. Separation efficiency of membrane in biotechnology: an experimental and mathematical study of flux control. *Chem. Eng. Sci.*, 47, 271-279.

McDonogh, R.M., Bauser, H., Stroh, N., Grauschopf, U., 1995. Experimental in situ measurement of concentration polarisation during ultra- and micro-filtration of bovine serum albumin and dextran blue solutions. *J. Membr. Sci.*, 104, 51-63.

Mendret, J., Guigui, C., Schmitz, P., Cabassud, C., 2009. Chapter 11: Optical and Acoustic Methods for in situ Characterization of Membrane Fouling. *Monitoring and visualizing membrane-based processes*. Edited by Güell et al., WILEY-VCH Verlag GmbH & Co. KGaA, Germany.

Mersmann, A., 1995. Purification of waste water in the chemical industry. *Chem. Eng. Process.*, 34, 279-282.

Metters, A.T., 1996. Master's Thesis: *Use of acoustic time-domain-reflectometry for real-time measurement of polymeric thin-film solidification*. University of Colorado, USA.

Mizrahi, G., Wong, K., Lu, X., Kujundzic, E., Greenberg, A.R., Gilron, J., 2012. Ultrasonic sensor control of flow reversal in RO desalination. Part 2: Mitigation of calcium carbonate scaling. *J. Membr. Sci.*, 419-420, 9-19.

Mores, W.D., Davis, R.H., 2001. Direct visual observation of yeast deposition and removal during microfiltration. *J. Membr. Sci.*, 189, 217-230.

Mores, W.D., Davis, R.H., 2002. Direct observation of membrane cleaning via rapid backpulsing. *Desalination*, 146, 135-140.

Mores, W.D., Davis, R.H., 2002. Yeast foulant removal by backpulses in crossflow microfiltration. *J. Membr. Sci.*, 208, 389-404.

Mulder, M., 1991. *Basic princibles of membrane technology*. Springer, Netherlands.

Nielsen, L.E., Landel, R.F., 1994. *Mechanical properties of polymers and composites*. Marcel Dekker Inc., USA.

Nordvang, R.T., Luo, J., Zeuner, B., Prior, R., Andersen, M.F., Mikkelsen, J.D., Meyer, A.S., Pinelo, M., 2014. Separation of 30-sialyllactose and lactose by nanofiltration: A trade-off between charge repulsion and pore swelling induced by high pH. *Sep. Purif. Technol.*, 138, 77-83.

Nunes, S.P., Peinemann, K.V., 2006. Part I: Membrane materials and membrane preparation. In book: *Membrane technology in the chemical industry*. WILEY-VCH Verlag GmbH & Co. KGaA, Germany.

Nyström, M., Mänttäri, M., 2009. Chapter 1: Introduction: Opportunities and Challenges of Real Time Monitoring on Membrane Processes. *Monitoring and visualizing membrane-based processes*. Edited by Güell et al., WILEY-VCH Verlag GmbH & Co. KGaA, Germany.

Okamoto, Y., Ohomori, K., Glatz, C.E., 2001. Harvest time effects on membrane cake resistance of Escherichia coli broth. *J. Membr. Sci.*, 190, 93-106.

Park, J.-S., Chilcott, T.C., Coster, H.G.L., Moon, S.-H., 2005. Characterization of BSA-fouling of ion-exchange membrane systems using a subtraction technique for lumped data. *J. Membr. Sci.*, 246, 137-144.

Park, J.-S., Choi, J.-H., Yeon, K.-H., Moon, S.-H., 2006. An approach to fouling characterization of an ion-exchange membrane using current-voltage relation and electrical impedance spectroscopy. *J. Colloid Interf. Sci.*, 294, 129-138.

Pendergast, M.T.M., Nygaard, J.M., Ghosh, A.K., Hoek, E.M.V., 2010. Using nanocomposite materials technology to understand and control reverse osmosis membrane compaction. *Desalination*, 261, 255-263.

Persson, K.M., Gekas, V., Trägårdh, G., 1995. Study of membrane compaction and its influence on ultrafiltration water permeability. *J. Membr. Sci*., 100, 155-162.

Pervov, A.G., Reztsov, Y.V., Milovanov, S.B., Koptev, V.S., 1996. Treatment of natural water by membranes. *Desalination*, 105, 33-39.

Peterson, R.A., 1996. Use of acoustic TDR to assess the effect of crosslinking on membrane compaction. *Master's thesis*. University of Colorado.

Peterson, R.A., Greenberg, A.R., Bond, L.J., Krantz, W.B., 1998. Use of ultrasonic TDR for real-time noninvasive measurement of compressive strain during membrane compaction. *Desalination*, 116, 115-122.

Pignon, F., Magnin, A., Piau, J.-M., Cabane, B., Aimar, P., Meireles, M., Lindner, P., 2000. Strctural characterization of deposits formed during frontal filtration. *J. Membr. Sci.*, 174, 189-204.

Pope, J.M., Yao, S., Fane, A.G., 1996. Quantitative measurements of the concentration polarization layer thickness in membrane filtration of oil-water emulsions using NMR micro-imaging. *J. Membr. Sci.*, 118, 247-257.

Porter, M.C., 1990. Chapter 3: Ultrafiltration. In book: *Handbook of industrial membrane technology*. Noyes publications, USA.

Reichert, U., Linden, T., Belfort, G., Kula, M-R., Thömmes, J., 2002. Visualising protein adsorption to ion-exchange membranes by confocal microscopy. *J. Membr. Sci.*, 199, 161-166.

Reinsch, V.E., Greenberg, A.R., Kelley, S.S., Peterson, R., Bond, L.J., 2000. A new technique for the simultaneous, real-time measurement of membrane compaction and performance during exposure to high-pressure gas. *J. Membr. Sci.*, 171, 217-228.

Remigy, J.-C., 2009. Chapter 10: X-ray Tomography Application to 3D Characterization of Membranes. *Monitoring and visualizing membrane-based processes*. Edited by Güell et al., WILEY-VCH Verlag GmbH & Co. KGaA, Germany.

Ren, J., Wang, R., 2011. Chapter 2: Preparation of polymeric membranes. In book: *Handbook of Environmental Engineering – Vol. 13: Membrane and Desalination Technologies*. Edited by Wang et al., Springer, USA.

Ripperger, S., Altmann, J., 2002. Crossflow microfiltration – state of the art. *Sep. Purif. Technol.*, 26, 19-31.

Roig, F., Dantras, E., Dandurand, J., Lacabanne, C., 2011. Influence of hydrogen bonds on glass transition and dielectric relaxations of cellulose. *J. Phys. D-Applied Physics*, 44.

Sanderson, M.L., Yeung, H., 2002. Guidelines for the use of ultrasonic non-invasive metering techniques. *Flow Measurement and Instrumentation*, 13, 125–142.

Sanderson, R., Li, J., Hallbauer, D.K., Sikder, S.K., 2005. Fourier wavelets from ultrasonic spectra: A new approach for detecting the onset of fouling during microfiltration of paper mill effluent. *Enivron. Sci. Technol*., 39, 7399-7305.

Sanderson, R., Li, J., Koen, L.J., Lorenzen, L., 2002. Ultrasonic time-domain reflectometry as a non-destructive instrumental visualization technique to monitor inorganic fouling and cleaning on reverse osmosis membranes. *J. Membr. Sci*., 207, 105-117.

She, Q., Wang, R., Fane, A.G., Tang, C.Y., 2016. Membrane fouling in osmotically driven membrane processes: A review. *J. Membr. Sci.*, 499, 201–233.

Silalahi, S.H.D., Leiknes, T., Ali, J., Sanderson, R., 2009. Ultrasonic time domain reflectometry for investigation of particle size effect in oil emulsion separation with crossflow microfiltration. *Desalination*, 1-3, 143-151.

Sim, L.N., Wang, Z.J., Gu, J., Coster, H.G.L., Fane, A.G., 2013. Detection of reverse osmosis membrane fouling with silica, bovine serum albumin and their mixture using in-situ electrical impedance spectroscopy. *J. Membr. Sci.*, 443, 45-53.

Sim, S.T.V., Chong, T.H., Krantz, W.B., Fane, A.G., 2012. Monitoring of colloidal fouling and its associated metastability using Ultrasonic Time Domain Reflectometry. *J. Membr. Sci.*, 401-402, 241-253.

Sim, S.T.V., Krantz, W.B., Chong, T.H., Fane, A.G., 2015. Online monitor for the reverse osmosis spiral wound module — Development of the canary cell. *Desalination*, 368, 48-59.

Sim, S.T.V., Suwarno, S.R., Chong, T.H., Krantz, W.B., Fane, A.G., 2013. Monitoring membrane biofouling via ultrasonic time-domain reflectometry enhanced by silica dosing. *J. Membr. Sci.*, 428, 24-37.

Sim, S.T.V., Tehari, A.H., Chong, T.H., Krantz, W.B., Fane, A.G., 2014. Colloidal metastability and membrane fouling – Effects ofcrossflow velocity, flux, salinity and colloid concentration. *J. Membr. Sci.*, 469, 174-187.

Solichien, M.S., O'Brien, D., Hammond, E.G., Glatz, C.E., 1995. Membrane-based extractive fermentation to produce propionic and acetic acids: Toxicity and mass transfer considerations. *Enzyme Microb. Tech.*, 17, 23-31.

Su, T.J., Lu, J.R., Cui, Z.F., Bellhouse, B.J., Thomas, R.K., Heenan, R.K., 1999. Identification of the location of protein fouling on ceramic membranes under dynamic filtration conditions. *J. Membr. Sci.*, 163, 265-275.

Su, T.J., Lu, J.R., Cui, Z.F., Thomas, R.K., 2000. Fouling of ceramic membranes by albumins under dynamic filtration conditions. *J. Membr. Sci.*, 173, 167-178.

Su, T.J., Lu, J.R., Cui, Z.F., Thomas, R.K., Heenan, R.K., 1998. Application of small angle neutron scattering to the in situ study of protein fouling on ceramic membranes. *Langmuir*, 14, 5517-5520.

Taheri, A.H., Sim, S.T.V., Sim, L.N., Chong, T.H., Krantz, W.B., Fane, A.G., 2013. Development of a new technique to predict reverse osmosis fouling. *J. Membr. Sci.*, 448, 12-22.

Touffet, A., Baron, J., Welte, B., Joyeux, M., Teychene, B., Gallard, H., 2015. Impact of pretreatment conditions and chemical ageing on ultrafiltration membrane performances. Diagnostic of a coagulation/adsorption/filtration process. *J. Membr. Sci.*, 489, 284-291.

Tung, K.-L., 2009. Chapter 15: Monitoring technique for water treatment membrane processes. *Monitoring and visualizing membrane-based processes*. Edited by Güell et al., WILEY-VCH Verlag GmbH & Co. KGaA, Germany.

Tung, K.-L., Damodar, H.-R., Damodar, R.-A., Wu, T.-T., Li, Y.-L., Lin, N.-J., Chuang, C.-J., You, S.-J., Hwang, K.-J., 2012. Online monitoring of particle fouling in a submerged membrane filtration system using a photointerrupt sensor array. *J. Membr. Sci.*, 407-480, 58-70.

Tung, K.-L., Wang, S., Lu, W.-M., Pan, C.-H., 2001. In situ measurement of cake thickness distribution by a photointerrupt sensor. *J. Membr. Sci.*, 190, 57-67.

Uchymiak, M., Rahardianto, A., Lyster, E., Glater, J., Cohen, Y., 2007. A novel ex situ scale observation detector (EXSOD) for mineral scale characterization and early detection. *J. Membr. Sci.*, 291, 86-95.

Uchymiak, M., Bartman, A.R., Daltrophe, N., Weissman, M., Gilron, J., Christofides, P.D., Kaiser, W.J., Cohen, J., 2009. Brackish water reverse osmosis (BWRO) operation in feed flow reversal mode using an ex situ scale observation detector (EXSOD). *J. Membr. Sci.*, 341, 60-66.

Vrouwenvelder, J.S., Bakker, S.M., Wessels, L.P., van Paassen, J.A.M., 2007. The Membrane Fouling Simulator as a new tool for biofouling control of spiral-wound membranes. *Desalination*, 204, 170–174.

Vrouwenvelder, J.S., Buiter, J., Riviere, M., van der Meer, W.G.J., van Loosdrecht, M.C.M., Kruithof, J.C., 2010. Impact of flow regime on pressure drop increase and biomass accumulation and morphology in membrane systems. *Water research*, 44, 689–702.

Vrouwenvelder, J.S., Graf von der Schulenburg, D.A., Kruithof, J.C., Johns, M.L., van Loosdrecht, M.C.M., 2009a. Biofouling of spiral-wound nanofiltration and reverse osmosis membranes: A feed spacer problem. *Water research*, 43, 583–594.

Vrouwenvelder, J.S., van Loosdrecht, M.C.M., Kruithof, J.C., 2011a. A novel scenario for biofouling control of spiral wound membrane systems. *Water research*, 45, 3890-3898.

Vrouwenvelder, J.S., van Loosdrecht, M.C.M., Kruithof, J.C., 2011b. Early warning of biofouling in spiral wound nanofiltration and reverse osmosis membranes. *Desalination*, 265, 206–212.

Vrouwenvelder, J.S., van Paassen, J.A.M., van Agtmaal, J.M.C., van Loosdrecht, M.C.M., Kruithof, J.C., 2009b. A critical flux to avoid biofouling of spiral wound nanofiltration and reverse osmosis membranes: Fact or fiction?. *J. Membr. Sci.*, 326, 36–44.

Vrouwenvelder, J.S., van Paassen, J.A.M., Wessels, L.P., van Dam, A.F., Bakker, S.M., 2006. The Membrane Fouling Simulator: A practical tool for fouling prediction and control. *J. Membr. Sci.*, 281, 316–324.

Ward, I.M., 1971. *Mechanical Properties of Solid Polymers*. John Wiley & Sons Ltd., England.

Weigel, T., Solomaier, T., Wehmayer, S., Peuker, A., Wolff, M.W., Reichl, U., 2016. A membrane-based purification process for cell culture-derived influenza A virus. *J. Biotechnol.*, 220, 12-20.

Wineman, A.S., Rajagopal, K.R., 2000. *Mechanical Response of Polymers*. Cambridge University Press, UK.

Xu, X., Li, J., Li, H., Cai, Y., Cao, Y., He, B., Zhang, Y., 2009. Non-invasive monitoring of fouling in hollow fiber membrane via UTDR. *J. Membr. Sci.*, 326, 103-110.

Yang, H., Fridjonsson, E.O., Johns, M.L., Wang, R., Fane, A.G., 2014. A non-invasive study of flow dynamics in membrane distillation hollow fiber modules using low-field nuclear magnetic resonance imaging (MRI). *J. Membr. Sci.*, 451, 46-54.

Yao, S., Costello, M., Fane, A.G., Pope, J.M., 1995. Non-invasive observation of flow profiles and polarization layers in hollow fibre membrane filtration modules using NMR micro-imaging. *J. Membr. Sci.*, 99, 207-216.

Yao, S., Fane, A.G., Pope, J.M., 1997. An investigation of the fluidity of concentration polarization layers in crossflow membrane filtration of an oil-water emulsion using chemical shift selective flow imaging. *Magn. Reson. Imaging.*, 15,235-242.

Yeo, S., Yang, P., Fane, A.G., White, T., Moser, H.O., 2005. Non-invasive observation of external and internal deposition during membrane filtration by X-ray microimaging (XMI). *J. Membr. Sci.*, 250, 189-193.

Zabkova, M., Borges da Silva, E.A., Rodrigues, A.E., 2007. Recovery of vanillin from lignin/vanillin mixture by using tubular ceramic ultrafiltration membranes. *J. Membr. Sci.*, 301, 221-237.

Zhang, Z., Bright, V.M., Greenberg, A.R., 2006. Use of capacitive microsensors and ultrasonic time-domain reflectometry for in-situ quantification of concentration polarization and membrane fouling in pressure-driven membrane filtration. *SENSOR ACTUAT B-CHEM*, 117, 323-331.

Zhang, Zh.-X., Greenberg, A.R., Krantz, W.B., Chai, G.-Y., 2003. Chapter 4: Study of membrane fouling and cleaning in spiral wound modules using ultrasonic time-domain reflectometry. In book: *Membrane Science and Technology – Vol. 8: New Insights into Membrane Science and Technology: Polymeric and Biofunctional Membranes*. Edited by Bhattacharyya, D. and Butterfield, D.A., Elsevier Science B.V., The Netherlands.

Zhao, K., Zhang, X., Wei, J., Li, J., Zhou, X., Liu, D., Liu, Z., Li, J., 2015. Calcium alginate hydrogel filtration membrane with excellent anti-fouling property and controlled separation performance. *J. Membr. Sci.*, 492, 536-546.

Publication I

Stade, S., Kallioinen, M., Mänttäri, M., Tuuva, T.

High Precision UTDR Measurements by Sonic Velocity Compensation with Reference Transducer

Reprinted with permission from

Sensors

Vol. 14, pp. 11682-11690, 2014

Publication II

Stade, S., Hakkarainen, T., Kallioinen, M., Mänttäri, M., Tuuva, T.

A Double Transducer for High Precision Ultrasonic Time-Domain Reflectometry Measurements

Reprinted with permission from

Sensors

Vol. 15, pp. 15090-15100, 2015

Publication III

Stade, S., Kallioinen, M., Mikkola, A., Tuuva, T., Mänttäri, M.

Reversible and irreversible compaction of ultrafiltration membranes

Reprinted with permission from

Separation and Purification Technology

Vol. 118, pp. 127-134, 2013

Publication IV

Stade, S., Kallioinen, M., Tuuva, T., Mänttäri, M.

Compaction and its effect on retention of ultrafiltration membranes at different temperatures

Reprinted with permission from
Separation and Purification Technology
Vol. 151, pp. 211-217, 2015

ACTA UNIVERSITATIS LAPPEENRANTAENSIS

732. LAMPINEN, MATTI. Development of hydrometallurgical reactor leaching for recovery of zinc and gold. 2016. Diss.

733. SUHOLA, TIMO. Asiakaslähtöisyys ja monialainen yhteistyö oppilashuollossa: oppilashuoltoprosessi systeemisenä palvelukokonaisuutena. 2017. Diss.

734. SPODNIAK, PETR. Long-term transmission rights in the Nordic electricity markets: An empirical appraisal of transmission risk management and hedging. 2017. Diss.

735. MONTONEN, JUHO. Integrated hub gear motor for heavy-duty off-road working machines – Interdisciplinary design. 2017. Diss.

736. ALMANASRAH, MOHAMMAD. Hot water extraction and membrane filtration processes in fractionation and recovery of value-added compounds from wood and plant residues. 2017. Diss.

737. TOIVANEN, JENNI. Systematic complaint data analysis in a supply chain network context to recognise the quality targets of welding production. 2017. Diss.

738. PATEL, GITESHKUMAR. Computational fluid dynamics analysis of steam condensation in nuclear power plant applications. 2017. Diss.

739. MATTHEWS, SAMI. Novel process development in post-forming of an extruded wood plastic composite sheet. 2017. Diss.

740. KÄHKÖNEN, TOMMI. Understanding and managing enterprise systems integration. 2017. Diss.

741. YLI-HUUMO, JESSE. The role of technical dept in software development. 2017. Diss.

742. LAYUS, PAVEL. Usability of the submerged arc welding (SAW) process for thick high strength steel plates for Arctic shipbuilding applications. 2017. Diss.

743. KHAN, RAKHSHANDA. The contribution of socially driven businesses and innovations to social sustainability. 2017. Diss.

744. BIBOV, ALEKSANDER. Low-memory filtering for large-scale data assimilation. 2017. Diss.

745. ROTICH, NICOLUS KIBET. Development and application of coupled discrete and continuum models in solid particles classification. 2017. Diss.

746. GAST, JOHANNA. The coopetition-innovation nexus: Investigating the role of coopetition for innovation in SMEs. 2017. Diss.

747. KAPOOR, RAHUL. Competition and disputes in the patent life cycle. 2017. Diss.

748. ALI-MARTTILA, MAAREN. Towards successful maintenance service networks – capturing different value creation strategies. 2017. Diss.

749. KASHANI, HAMED TASALLOTI. On dissimilar welding: a new approach for enhanced decision-making. 2017. Diss.

750. MVOLA BELINGA, ERIC MARTIAL. Effects of adaptive GMAW processes: performance and dissimilar weld quality. 2017. Diss.

751. KARTTUNEN, JUSSI. Current harmonic compensation in dual three-phase permanent magnet synchronous machines. 2017. Diss.

752. SHI, SHANSHUANG. Development of the EAST articulated maintenance arm and an algorithm study of deflection prediction and error compensation. 2017. Diss.

753. CHEN, JIE. Institutions, social entrepreneurship, and internationalization. 2017. Diss.

754. HUOTARI, PONTUS. Strategic interaction in platform-based markets: An agent-based simulation approach. 2017. Diss.

755. QU, BIN. Water chemistry and greenhouse gases emissions in the rivers of the "Third Pole" / Water Tower of Asia". 2017. Diss.

756. KARHU, PÄIVI. Cognitive ambidexterity: Examination of the cognitive dimension in decision-making dualities. 2017. Diss.

757. AGAFONOVA, OXANA. A numerical study of forest influences on the atmospheric boundary layer and wind turbines. 2017. Diss.

758. AZAM, RAHAMATHUNNISA MUHAMMAD. The study of chromium nitride coating by asymmetric bipolar pulsed DC reactive magnetron sputtering. 2017. Diss.

759. AHI, MOHAMADALI. Foreign market entry mode decision-making: Insights from real options reasoning. 2017. Diss.

760. AL HAMDI, ABDULLAH. Synthesis and comparison of the photocatalytic activities of antimony, iodide and rare earth metals on SnO2 for the photodegradation of phenol and its intermediates under UV, solar and visible light irradiations. 2017. Diss.

761. KAUTTO, JESSE. Evaluation of two pulping-based biorefinery concepts. 2017. Diss.

762. AFZALIFAR, ALI. Modelling nucleating flows of steam. 2017. Diss.

763. VANNINEN, HEINI. Micromultinationals - antecedents, processes and outcomes of the multinationalization of small- and medium-sized firms. 2017. Diss.

764. DEVIATKIN, IVAN. The role of waste pretreatment on the environmental sustainability of waste management. 2017. Diss.

765. TOGHYANI, AMIR. Effect of temperature on the shaping process of an extruded woodplastic composite (WPC) profile in a novel post-production process. 2017. Diss.

766. LAAKKONEN, JUSSI. An approach for distinct information privacy risk assessment. 2017. Diss.

767. KASURINEN, HELI. Identifying the opportunities to develop holistically sustainable bioenergy business. 2017. Diss.

768. KESKISAARI, ANNA. The impact of recycled raw materials on the properties of woodplastic composites. 2017. Diss.

769. JUKKA, MINNA. Perceptions of international buyer-supplier relational exchange. 2017. Diss.

770. BAYGILDINA, ELVIRA. Thermal load analysis and monitoring of doubly-fed wind power converters in low wind speed conditions. 2017. Diss.